ASTRONOMY & ASTROPHYSICS
SUPPLEMENT SERIES

SEPTEMBER 1989, PAGE 359

Astron. Astrophys. Suppl. Ser. **79**, 359-383 (1989)

The winds of O-stars. I. an analysis of the UV line profiles with the SEI method

M. A. T. Groenewegen ([1]) and H. J. G. L. M. Lamers ([1, 2, 3])

([1]) SRON Laboratory for Space Research, Beneluxlaan 21, NL-3527 HS, Utrecht, The Netherlands
([2]) Astronomical Institute at Utrecht, Princetonplein 5, NL- 3584 CC, Utrecht, The Netherlands
([3]) Joint Institute for Laboratory Astrophysics, University of Colorado and National Bureau of Standards, Boulder, CO 80309-0440, U.S.A.

Received February 13, accepted March 17, 1989

Summary. — We present the results of a study of the C IV, N V, Si IV, C III, and N IV ultraviolet P Cygni profiles of 26 O-type stars and one B star. The profiles observed with the IUE satellite are compared with theoretical profiles calculated with the SEI-method. The effects of turbulence in the wind, limb darkening, photospheric lines and interstellar Ly α are taken into account. The profile fits are very accurate and show a significant improvement compared to previously obtained fits with the Sobolev method. The terminal velocities are about 15 percent smaller than those previously derived from Sobolev line fits. The velocity law can be described by $\beta = 0.68 \pm 0.15$, which is steeper than derived from IR studies and agrees reasonably well with the values of β predicted by the radiation driven wind theory. The column densities of the observed ions are compared with those derived from Sobolev line fits. The differences are typically a factor 3 to 10, with systematic differences between the analysis of the same stars by different authors. The consequences for the determination of the mass loss rates from O-stars are discussed. The values of $\dot{M}q$ at $v = 0.5\, v_\infty$ are derived for all ions. The interstellar HI column densities are derived from the Ly α wings in the profiles of the N V resonance lines. We find a mean ratio of $N_{\rm HI} = (3.8 \pm 0.9) \times 10^{21}\, E(B-V)$ for the lines of sight to our program stars.

Key words: circumstellar matter — early type stars — line profiles — mass loss — stellar winds — ultraviolet lines.

1. Introduction.

The best indications of mass loss from hot stars are the UV resonance lines, whose profiles are very sensitive to the presence of a stellar wind and its characteristics. Unfortunately, these profiles are not the most *accurate* indicators of the mass loss rates, because their analysis is subject to large uncertainties in the degree of ionization in the winds. The most accurate mass loss indicator is the radio free-free emission from stellar winds, which however can be observed for a small number of nearby stars only. The infrared excess and the Hα emission can be observed in many O-stars, but their interpretation depends critically on the density and velocity structure in the lower parts of the wind which is not well known (see e.g., Lamers, 1988 for a review of the methods and the uncertainties). For this reason our knowledge on the mass loss from O-stars and its effects on the evolution of massive stars is predominantly based on the studies of the UV resonance lines.

Numerous studies have been devoted to the determination of the mass loss rates from early-type stars by means of the quantitative study of the P Cygni profiles of the UV resonance lines. In these studies the observed profiles are compared with theoretical profiles which are calculated for spherically symmetric and stationary stellar winds for which the velocity law and the distribution of the absorbing atoms are specified. By comparing the observations with a grid of theoretical profiles of various velocity laws and particle distributions one may select the best agreement and conclude

Send offprint requests to: H. J. G. L. M. Lamers, SRON Laboratory for Space Research, Beneluxlaan 21, NL-3527 HS Utrecht, The Netherlands.

that the parameters which describe the best-fitting theoretical profiles apply to the star whose mass loss one tries to determine. This technique was first applied by Lamers and Morton (1976) and Lamers and Rogerson (1978) and later by e.g., Hamann (1980 and 1981b), Gathier *et al.* (1981), Olson and Castor (1981), Garmany *et al.* (1981), Prinja and Howarth (1986) and Howarth and Prinja (1988). All these studies (except Hamann's) were based on line profile calculations in the Sobolev approximation, i.e. the intrinsic width of the absorption component is neglected relative to the Doppler velocities in the wind (Sobolev, 1958 ; Castor, 1970).

During recent years, it has become clear, however, that the Sobolev approximation may not be valid for the study of the winds of early-type stars. There is increasing evidence that some kind of broadening mechanism is effective which may increase the width of the intrinsic absorption from a few km/s to a few hundred km/s. The major evidence for these effects is found in the detailed studies of a few stars such as τ Sco (Lamers and Rogerson, 1978 ; Hamann, 1981b) and ζ Pup (Hamann, 1980) and in the presence of wide absorption troughs in the UV reasonance lines of most early type stars with strong mass loss. Lucy (1984) has proposed that these troughs are due to a non-homogeneous velocity law in a wind which is perturbed by shocks. Lamers *et al.* (1987) have shown that the troughs can also be explained by "turbulence" in the winds.

The presence of shocks or turbulence in the winds will alter the line profiles compared to the Sobolev profiles in three ways : it produces wide absorption troughs in saturated lines, it shifts the emission peak of the P Cygni profiles to longer wavelengths, and it produces a gradual slope in the violet absorption edge of the saturated P Cygni profiles (Lamers *et al.*, 1987). These three effects are commonly observed in the UV resonance lines of O-stars. In fact they are the major discrepancies between the observed line profiles and the theoretical profiles of the Sobolev line fitting studies (see e.g., Garmany *et al.*, 1981).

The failure of the Sobolev line fitting technique in the studies of the winds of O-stars indicates that the results derived from this fitting may be in error. One obvious error is a systematic overestimate of the terminal velocities of the stellar winds by about 400 km/s (Groenewegen *et al.*, 1989, Paper II). The other error is a possible overestimate of the column densities and the distribution of the absorbing ions in the wind. This may result in errors in the mass loss rates and in the empirical ionization ratios.

In an attempt to correct the errors in the mass loss rates, velocity laws and ionization in the wind determined by the Sobolev-method, and in the hope of improving our knowledge about mass loss from O-stars, we have studied the P Cygni profiles of the UV lines of 26 O-stars, and one early-B star observed with IUE and compared them with theoretical profiles in which the effect of line-broadening was taken into account. The profiles are calculated with the SEI method (Lamers *et al.*, 1987) which allows the introduction of turbulent broadening in the wind. This method has the simplicity and efficiency of the Sobolev-method and an accuracy comparable to that of the physically more correct Comoving Frame Method (Mihalas *et al.*, 1975).

In this paper we present the method, the line fitting analysis and the results in terms of column densities and distribution of absorbing atoms, and the velocity laws. The results of this study on the terminal velocities of the stellar winds are described by Groenewegen *et al.* (1989, Paper II). The derived ionization of the winds will be compared with predicted ionizations in order to derive accurate mass loss rates by Groenewegen and Lamers (1989, Paper III).

2. Observations and stellar data.

The high resolution IUE spectra were taken from the International Ultraviolet Explorer atlas of O-type spectra from 1200 to 1900 Å by Walborn *et al.* (1985). Both printed version and the magnetic tape version (1149.00 to 1949.75 Å) were used. For the details of the data in this atlas we refer to Walborn *et al.*. In short, they retrieved the IUE Spectral Image Processing System (IUESIPS) data from the data archive. The background was smoothened and subtracted. A ripple-correction was applied to adjust for systematic variations along each order caused by varying efficiency of the echelle grating. The spectrum resampled to an uniform resolution of 0.25 Å, which corresponds to a resolution of 50 km/s at 1500 Å. Finally the resampled spectrum was rescaled to locate an approximate continuum for convenient plotting.

From the 98 stars in the atlas we selected 27. The following criteria were used : the profiles should have well developed P Cygni profiles and unnecessary duplication in spectral type was avoided. For example if there were five O6V stars in the atlas only one or two were selected. The program stars are listed in table I, together with their basic data. The compilation of these data has been described in Paper II. The values of $E(B-V)$, are derived from the intrinsic colors by Schmidt-Kaler (1982) and the observed colors from Garmany (1987). The adopted temperature scale and the Bolometric Corrections are from Chlebowski and Garmany (1988), based on non-LTE studies of a number of O-stars. The absolute visual magnitudes are from the compilation by Garmany (1987) which is predominantly based on cluster membership. The masses are derived from $T_{\rm eff}$ and L and the evolutionary tracks of Maeder and Meynet (1987). We assumed that the stars are moving away from the main-sequence, rather than returning from the red supergiant phase. The radii are derived from L and $T_{\rm eff}$. The gravity, not corrected for radiation pressure, and the escape velocity corrected for radiation pressure by electron scattering are also given. The uncertainties listed in table I are based on an assumed uncertainty of $\Delta M_{\rm bol} = 0.2$ and $\Delta \log T_{\rm eff} = 0.02$ (Paper II). The uncertainties listed in table I are maximum deviations from the adopted values, rather than standard errors.

3. The method used for the profile fitting.

3.1 THEORETICAL LINE PROFILES. — The traditional methods for the calculation of line profiles, i.e. the Sobolev method and the Comoving Frame Method (CFM), both have their drawbacks. The Sobolev method is simple to use but is only accurate when the velocity gradient is large and the CF method is very accurate but is very elaborate. The SEI method combines both accuracy and simplicity (Lamers *et al.*, 1987). We will recall the most important principles and formulae of the SEI method.

The Sobolev approximation is only valid when the velocity gradient, $\mathrm{d}v/\mathrm{d}r$, is much larger than v_t/ℓ, where v_t represents a turbulent motion and ℓ is a characteristic lengthscale over which the density changes. It has become clear that (large) turbulent motions occur in stellar winds. Therefore the Sobolev approximation is not valid in the lower layers of the wind where the velocity changes from subsonic to supersonic, and at large distances from the star where the velocity becomes constant.

Hamann (1981a) has compared the Sobolev method and CF method and concluded that the main discrepancy lay in the exact integration of the transfer equation and only to a small extent in the calculation of the source function. In the SEI method the source function is calculated in the Sobolev approximation while the transfer equation is solved exactly. This makes it possible to calculate line profiles in a spherically symmetric expanding wind with a monotonically increasing velocity, in which chaotic motions act as "turbulence". The profile of this turbulence is assumed to be isotropic and Gaussian with a constant width v_{turb}.

The radiative transfer equation is solved in the wind only. The photosphere is considered to be a lower boundary condition. Its spectrum is a continuum with or without an absorption line at the rest wavelength of the line whose profile is to be calculated. This separation between photosphere and the wind could produce errors, but a comparison of the SEI profiles with the CMF profiles leads to the conclusion that these errors are very small (Lamers *et al.*, 1987). The calculations of doublets is more complicated than the case of a single line, because photons which are scattered or emitted by one component may interact at another place in the wind with the other component. In a spherically expanding wind with monotonically increasing velocity all atoms move away from each other. Therefore a photon emitted by the red component cannot be absorbed again, but a photon emitted or scattered by the blue component can be absorbed elsewhere in the wind but only by an atom whose velocity relative to the emitting atom corresponds to the wavelength difference between the doublet components. This means that the source function of the red component is changed by the presence of the blue one, but not vice versa. This problem of "radiatively coupled points" for doublet lines is solved exactly in the SEI method.

The stellar wind is specified by two functions : the radial optical depth $\tau(v)$ and the velocity law $v(r)$. The velocity in the wind is normalized to the terminal velocity, v_∞ :

$$w(r) = v(r)/v_\infty , \tag{1}$$

and the distance r is normalized to the photospheric radius R :

$$x = r/R. \tag{2}$$

The adopted velocity law is of the type :

$$w(x) = w_0 + (1 - w_0)\,(1 - 1/x)^\beta , \tag{3}$$

where w_0 is the normalized velocity at the photosphere, for which we adopt a value of $w_0 = 0.01$. The free parameter β describes the steepness of the velocity law. The detailed models of radiation driven winds (Pauldrach *et al.*, 1986) show that β is expected to be about 0.8 for stars with T_{eff} between 30000 and 50000 K.

The radial optical depth is defined by :

$$\begin{aligned}\tau(v) &= \frac{\pi e^2}{mc}\,(gf)_{\ell \mathrm{u}}\,\lambda_0\,(n_\ell/g_\ell - n_{\mathrm{u}}/g_{\mathrm{u}})\,(\mathrm{d}v/\mathrm{d}r)^{-1} \\ &= \frac{\pi e^2}{mc}\,(gf)_{\ell \mathrm{u}}\,\lambda_0\,(R_*/v_\infty)\,(n_\ell/g_\ell - n_{\mathrm{u}}/g_{\mathrm{u}})\,(\mathrm{d}w/\mathrm{d}x)^{-1}\end{aligned} \tag{4}$$

where f is the oscillator strength of the line, λ_0 is the rest wavelength, g the statistical weight and n is the ion number density. The subscripts ℓ and u refer to the lower and upper level of the transition. In some stars the blue wing of the UV lines formed in the wind do not extend to v_∞ or $w = 1$ but to a smaller velocity, w_1, with $w_1 \leq 1$. This effect can be included easily in the optical depth law. We adopt the following parametrization of the optical depth law :

$$\begin{aligned}\tau(w) &= (T/I)\,(w/w_1)^{\alpha 1}\left\{1 - (w/w_1)^{1/\beta}\right\}^{\alpha 2} \quad \text{for } w \leq w_1 \quad \text{and} \\ \tau(w) &= 0 \qquad\qquad\qquad\qquad\qquad\qquad\quad \text{for } w > w_1,\end{aligned} \tag{5}$$

where I is a normalization parameter

$$I = \int_{w_0}^{w_1} (w/w_1)^{\alpha_1} \left\{1 - (w/w_1)^{1/\beta}\right\}^{\alpha_2} \mathrm{d}w \qquad (6)$$

and T is integrated optical depth

$$T = \int_{w_0}^{1} \tau(w) \mathrm{d}w \qquad (7)$$

The choice of the optical depth law as in equation (5) is based on the following consideration. Equation (4) shows that $\tau \sim n(\mathrm{d}x/\mathrm{d}w)$, and equation (3) shows that $w \sim (1 - 1/x)^{\beta}$. Therefore $x \sim 1/(1 - w^{1/\beta})$ and $\mathrm{d}x/\mathrm{d}w \sim x^2\, w^{1/\beta - 1}$. From mass conservation we have $n \sim q/x^2 w$, where q is the ionization fraction. Assume that q varies like $x^{-s} w^{-t}$, then we find that $\tau \sim w^{\alpha_1}(1 - w^{1/\beta})^{\alpha_2}$ with $\alpha_1 = 1/\beta - 2 - t$ and $\alpha_2 = +s$. For constant ionization we expect $\alpha_1 = 1/\beta - 2$ and $\alpha_2 = 0$. For doublets we demand a ratio of the optical depth of the two components according to $T_{\mathrm{blue}} = T_{\mathrm{red}} (f\lambda_0)_{\mathrm{blue}}/(f\lambda_0)_{\mathrm{red}}$. T, α_1, α_2, and w_1 are free parameters. In the case of resonance lines, when the population of the upper level can be neglected, T is related to the column density $N_i(\mathrm{cm}^{-2})$ of the lower level of ion i :

$$T = (\pi e^2/mc)\, f\, \lambda_0\, N_i/v_\infty. \qquad (8)$$

We adopted a Gaussian shaped turbulence profile with a constant width. We did not complicate our model by assuming a radial dependence in the turbulent velocity. The main reason being that the scarce information available indicate that the turbulent velocity might be nearly constant throughout the wind. One might have expected that the turbulent motions might be smaller close the star than at larger distances because the flow velocity increases outwards. However, Lamers and Rogerson (1978) as well as Hamann (1981b) found a high turbulent motion even in the low velocity part of the wind of τ Sco, and Hamann (1980) found the same turbulent velocity in both the inner as well as the outer part of the wind of ζ Pup. A constant turbulent velocity is therefore a reasonable first approximation. The turbulence in the wind was assumed to be constant and isotropic, and is represented by a Gaussian broadening profile with a Doppler width of v_{turb}. This width is normalized to the terminal velocity by $w_{\mathrm{G}} = v_{\mathrm{turb}}/v_\infty$.

3.2 Limb darkening. — Castor and Lamers (1979) noticed that the effects of limb darkening on the predicted P Cygni profiles were small (< 0.5%) for both moderate and strong limb darkening, except close to the line center, where the difference could amount to 15% . They concluded that the effect of limb darkening is not important when observed and calculated profiles are compared with one another.

This conclusion is generally valid for the calculation of a profile in the Sobolev approximation because near the line center the Sobolev approximation breaks down anyway. With the SEI method however the profiles can be computed more accurately, also near the line center (see Lamers *et al.*, 1987), so it is important to include limb darkening in the calculation.

We adopt the following limb darkening law

$$I(\mu) = I_{\mathrm{c}} \left[1 - a(1 - \mu) - b(1 - \mu)^2\right], \qquad (9)$$

where $\theta = \arccos \mu$ is the angle between the direction to the observer and the radiation. The quadratic limb darkening coefficients a and b were calculated from the tables given by Wade and Rucinski (1985). They calculated linear and quadratic limb darkening coefficients for the model atmospheres of Kurucz (1979) at 11 wavelengths. We used the values calculated for the models with solar abundances and calculated a and b at the wavelengths 1362 and 1815 Å, because those were the two wavelengths which bracket our region of interest. We used linear interpolations and extrapolations in $\log g$ and T_{eff}, to derive a and b for each program star. Finally, we calculated the limb darkening coefficients at the rest wavelengths of the ions under consideration using linear interpolation in the wavelength between the values found at 1362 and 1815 Å. This interpolation is justified because the limb darkening coefficients are a smooth function of the wavelength for O-stars. The limb darkening coefficients a and b at both wavelengths are tabulated in table II.

The extent to which the inclusion of limb darkening changes the line profile can be seen in figure 1. We calculated a N IV profile for the following combinations $(a, b) = (0, 0)$, $(0.3, 0.2)$ and $(0.5, 0.5)$, corresponding to no limb darkening, a mean value and a maximum value for the limb darkening coefficients. Increasing the effect of limb darkening increases the emission. An increase in the emission can also be obtained by adopting a softer velocity law. Therefore the analyses of the observed profiles will result in slightly steeper velocity laws, i.e. smaller values of β when limb darkening is taken into account. The mathematical changes needed to incorporate limb darkening in the SEI method are described in appendix I.

3.3 Photospheric lines. — The possible presence of photospheric lines at the rest wavelengths of the P Cygni profiles was taken into account. We assumed that the photospheric profiles are due to a Gaussian absorption coefficient with an intrinsic width, normalized to v_∞ of w_{phot}, and a central opacity of A_{phot}. This implies that the photospheric spectrum, which is treated as a lower boundary for the solution of the transfer equation in the wind, is approximated by

$$I = \exp\left\{-A_{\mathrm{phot}} \exp\left(-w^2/w_{\mathrm{phot}}^2\right)\right\} \qquad (10)$$

for singlets and

$$I = \exp\left[-A^{\mathrm{B}}_{\mathrm{phot}} \exp\left(-w^2/w_{\mathrm{phot}}^2\right) - A^{\mathrm{R}}_{\mathrm{phot}} \exp\left\{-(w - \delta)^2/w_{\mathrm{phot}}^2\right\}\right] \qquad (11)$$

for doublets, where B and R refer to the blue and red components respectively and δ is the separation between the rest wavelengths of the components expressed in velocity normalized to v_∞

$$\delta = c\left(1 - \lambda_0^B/\lambda_0^R\right)/v_\infty \qquad (12)$$

Notice that we used the same intrinsic widths for w_{phot} for the red and blue component. The ratio A^B_{phot}/A^R_{phot} was assumed to be in agreement with the ratio of the values of gf of the two components, which is 2 for the resonance lines of N V, C IV and Si IV. We adopted the equations (10) and (11) because we expect $I \sim e^{-\tau}$ and $\tau \sim \phi$, where ϕ is the profile function which we assumed to be Gaussian.

For each star and each P Cygni profile the continuum was chosen by looking at each spectrum individually. The adopted continuum was not automatically determined by the highest points in the spectrum. It is more realistic to estimate the "effective" continuum entering into the stellar wind. When the spectrum on both sides of the line profile contained many and/or deep stellar lines adopted continuum was set at about 90 to 95% of the level determined by the highest points in the spectrum. The reason for this assumption is the fact that the P Cygni profiles result from scattering of photospheric radiation in the wind, and so the presence of many photospheric absorption lines will reduce the amount of radiation to be scattered in the wind.

3.4 INTERSTELLAR LINES. — Interstellar lines can be identified easily because they are deep and narrow. Walborn *et al.* (1985) provide a list of the most important interstellar lines in the region 1200 to 1900 Å. Because the interstellar lines are very narrow they hardly change the wind profile and no correction is needed. The only exception is the Ly α line at 1215.67 Å, which changes the blue wing of the N V line ($\lambda\lambda$ 1238, 1242 Å) substantially in most cases.

The following correction procedure was applied for the N V lines. After calculating the N V line profiles relative to the stellar continuum in the usual way, the fluxes were multiplied by $\exp\{-\tau(\lambda)\}$ to allow for the interstellar extinction by Ly α, where

$$\tau(\lambda) = \pi\,\lambda_0^2\,e^2\,f\,N_H\,\phi(\lambda)/\left(mc^2\right), \qquad (13)$$

and $\phi(\lambda)$ is the profile function given by:

$$\phi(\lambda) = (\Delta\lambda_H/2\pi)\left\{(\Delta\lambda)^2 + (\Delta\lambda_H/2)\right\}^{-1}, \qquad (14)$$

where $\Delta\lambda = \lambda - \lambda_0$, $\lambda_0 = 1215.67$ Å, $f = 0.4162$ and $\Delta\lambda_H = (\lambda_0^2/2\pi c)\,\gamma$ with $\gamma = \sum_{n<n'} A_{nn'}$ ($A_{nn'}$ is the Einstein coefficient) and N_H is the column density of neutral hydrogen. For Ly α this yields

$$\gamma = A_{21} = 8\,\pi^2\,e^2\,g_1\,f_{12}/\left(mc\,\lambda_0^2\,g_2\right) \qquad (15)$$

(see Rybicki and Lightman, 1979, page 367). Substituting equations (14) and (15) into (13) yields

$$\begin{aligned}\tau(\lambda) &= 4\,\pi\,e^2/(mc\gamma)f\,N_H/\left(1 + (2/\Delta\lambda_H)^2(\Delta\lambda)^2\right)\\ &= 7.0562\times10^{-11}\,N_H/\left(1 + 1.6574\times10^9(\Delta\lambda)^2\right)\end{aligned} \qquad (16)$$

where $\Delta\lambda$ is in Ångströms, and N_H in cm^2. This formula, without derivation, was already given by Jenkins (1971) and Bohlin (1973). In comparing the observed and the calculated N V profiles we can give an estimate for N_H. We will discuss the values we found for the neutral hydrogen column density in section 7.

3.5 NARROW ABSORPTION COMPONENTS. — The large amount of UV spectra that have become available with IUE has shown that spectral lines are variable on all timesticales. See for a recent review on this topic Henrichs (1988).

The following stars in our sample have been reported to show variability in at least one spectral line: ζ Pup, 15 mon, ξ Per, λ Ori A, α Cam, μ Nor, ι Ori, ξ Ori, ε Ori (see e.g., the survey by snow, 1977; Lamers *et al.*, 1982; and Prinja and Howarth, 1986).

We have not tried to identify narrow absorption components (NAC) in the spectra of our stars. The main reason is the fact that we only had one spectrum of each star, while we know that the presence of NAC is a strictly time dependent phenomenon. However these NAC can be modeled (see e.g., the review by Henrichs, 1988) and such a model could easily be incorporated in the SEI method. Although we did not explicitly identify NAC, the nature of the narrow absorption components (i.e., moderately deep and moderately wide absorption dips at a velocity between 0.5 and 1.0 times the terminal velocity superimposed on the P Cygni profile) made it possible to identify likely candidates. This enabled us to distinguish between the overall P Cygni profile, to be matched by the calculated profiles and the extra absorption dips caused by the narrow absorption components when making a line fit.

3.6 THE LINE FITS. — The lines studied in this paper are those of C III, C IV, N IV, N V, and Si IV. Their atomic data are given in table III (from Snow and Morton, 1976). We only tried to fit the lines which had well-developed P Cygni profiles. As mentioned before we fixed the initial

wind velocity w_0 at the representative value of 0.01. For one star we calculated a profile with w_0 being 0.001 and 0.03 but this made only an extremely small difference. Therefore w_0 is not a quantity that can be derived from the line fits.

When we started this work in the fall of 1986 the magnetic version of the atlas of Walborn *et al.* (1985) was not yet available. So we started using the printed version. The spectra were copied and enlarged. A continuum was chosen in the manner described in section 3.2, and a smooth curve was drawn through the data thereby neglecting possible Narrow Absorption Components. This was the curve to which the theoretical profiles were fitted.

Apart from an interactively working computer program, a batch version was written which minimized : $\chi^2 = \Sigma(1 - F_o/F_m)^2$, with F_o the observed and F_m the model flux, over all chosen wavelength points. Typically 15 to 25 wavelengths were chosen at which the fluxes were calculated. The value of χ^2 could be minimized to any combination of the following parameters : w_G, T, β, α_1, α_2.

In the first step an approximate value of v_∞, β and T were determined for each line individually, by using $w_G = 0.1$, $w_1 = 1$ and $\alpha_1 = \alpha_2 = 0$ and no photospheric lines. Then the batch program was used. This listed for each line the combination of w_G, T, β, α_1, α_2 that minimized χ^2. In this step we used an important constaint : the terminal velocity, the turbulent velocity and β are not free parameters for each line individually they must be the same for every line of one particular star. The final values of v_∞, w_G, and β were determined interactively. We estimated A_{phot} and w_{phot}. Then the batch version was used again but this time χ^2 was minimized to T, α_1, α_2 and for some lines to w_1. The terminal velocity, w_G, A_{phot}, w_{phot} and β were fixed. The values of T, α_1, α_2 given by the minimalization process were not automatically taken as the final values. Sometimes a certain combination could minimize χ^2 but would still produce an unsatisfactory fit. In those cases the fits were improved further by using the interactive program. We stress that we did not use χ^2 as a formal statistical parameter but merely as an indicator how one parameter would influence another. This made it also possible to estimate an error in the parameters.

Finally, the fits were plotted on top of the original spectra from the tape version and compared. In a minority of cases T was modified a bit and in some cases A_{phot} and/or w_{phot} were changed. The final fits are presented in the figures 2a to 2f. The parameters of the line fits are listed in table IV. The parameters of the adopted photospheric lines are listed in table V.

As the presence of a photospheric component in the observed P Cygni profiles depends strongly on the optical depth of wind-component, the values of A_{phot} cannot be considered as a reliable indication of the strength of a photospheric line. For instance if the P Cygni profile has a large optical depth, we did not need to adopt a photospheric component in the line fit procedure, even if a photospheric line is present. Only for the lines with optically thin P Cygni profiles, e.g., C III and N IV lines, are the values of A_{phot} indicative of the real strength of the photospheric lines.

In general, the predicted profiles agree very well with the observed profiles. In particular it is gratifying to see that most of the systematic differences between the Sobolev line fits and the observations are removed. Compare e.g., the Sobolev fits of the stars ζ Pup and α Cam obtained by Garmany *et al.* (1981) with our fits. The improvement is remarkable, especially in the prediction of the deep and wide absorption and in the shape and position of the emission peaks. Nevertheless, our predicted profiles do not match the observations in all cases equally well, but the differences are small.

The observed profiles of the saturated C IV lines and the saturated N V lines in some stars are slightly deeper at the long wavelength side of the absorption than the predicted profiles. This effect is most clearly seen for HD 36861, HD 93250, HD 101190 and HD 101436. This discrepancy could have been solved by adopting a larger turbulent velocity, which would extend the absorption to longer wavelength (Lamers *et al.*, 1987). However in that case the emission peak would shift to wavelengths longer than observed, and the violet absorption edge would be less steep. The discrepancy is possibly due to the effect that we adopted an isotropic turbulence with a constant width throughout the wind. This is of course a severe over-simplification, but considering our lack of knowledge of the true nature of the broadening in the winds by shocks or turbulence, we adopted this simplification. It is also possible that the small differences between the predictions and observations in some profiles are due to the fact that our adopted optical depth law (Eq. (5)) does not represent the true variation of $\tau(v)$ in the wind.

In view of the very good general agreement between the predicted and observed profiles we conclude that the velocity laws and the numerical values of $\tau(v)$ derived from our line fits are accurate and reliable. The uncertainty in $\tau(v)$ will depend on $\tau(v)$ itself. If we adopt, on the basis of the line fits, that the predictions fit the observations within about 20% , with a few exceptions, we find that the uncertainty in $\tau(v)$ is about $\Delta\tau(v) \simeq 0.20\, e^{\tau(v)}$. For highly saturated parts of the line where $\tau(v) \gtrsim 4$ the derived value of $\tau(v)$ is only on lower limit.

The resulting parameters of the velocity law, v_∞ and β, and the turbulent velocities v_{turb} are listed in table I, together with their uncertainties. For each star and each doublet the values of the optical depth parameters T_R, α_1, α_2, and w_1, are listed in table IV and the parameters of the photospheric lines A^R_{phot} and w_{phot}, with their estimated errors, are listed in table V.

3.7 THE ACCURACY OF THE DERIVED PARAMETERS. — In this section we will discuss the accuracy of the derived parameters T, α_1 and α_2 and justify the errors we attributed to them (see Tab. IV). We will do this taking the C IV profile of ζ Pup as

an example (Fig. 3). The saturated C IV line is shown in figure 3a. The solid line represents the adopted fit, with $T_R = 7.2$, $\alpha_1 = 0.97$ and $v_{turb} = 290$ km/s. The dotted line represents the fit with the optical depth increased to $T_R = 65$. The resulting profile has a wider absorption trough than the adopted one, and the emission peak has shifted to the right. This fit is not acceptable. However we can improve this fit lowering the turbulent velocity. The dashed line is a fit with $T_R = 65$, $\alpha_2 = 2$ and $v_{turb} = 200$ km/s, the same value used by Puls (1987) which is not excluded by our value of 290 ± 70 km/s. This fit, although with a larger χ^2 than our adopted fit, looks almost as good.

It is clear that given this lowest acceptable value of the turbulent velocity, we cannot increase T much further because then the trough would be too wide and the emission peak would shift too far right. We conclude that given the uncertainty in the turbulent velocity, the optical depth of saturated lines is between the lower limit quoted in table IV and about 20 times that value.

We stress that the adopted value of v_{turb} and its uncertainty is based on a study of the fits of *all* P Cygni profiles of each star.

In figure 3b we plotted several fits made for the unsaturated N IV line. Fortunately the turbulent velocity has a smaller impact on the shape of the profile than on a saturated line (not demonstrated in Fig. 3b), so the parameters T, α_1, α_2 can be derived quite accurately. To demonstrate this we plotted our adopted fit (solid line, $T = 2.3$, $\alpha_1 = 0.40$, $\alpha_2 = 3.5$) and fits with increased values of the parameters by 1σ ($T = 2.5$, dashed-dotted line) or 2σ ($\alpha_1 = 0.56$, dashed and $\alpha_2 = 4.3$, dotted). These changes in the parameters produce appreciable changes in the theoretical profiles.

3.8 A DISCUSSION OF THE GENERAL TRENDS. — We will now briefly discuss the fits and some special properties of the lines.

C IV 1548.19 and 1550.76 Å

The C IV resonance lines are saturated in almost all stars of luminosity class I, and in stars of class III with spectral types earlier than O7.5. The lines are not saturated in the later type stars of class III and in class V stars. The strength decreases from O7 V to later types.

There is a blend around 1533 Å. Two relative strong lines in that vincinity are a P II line at 1532.51 Å and a Fe V line at 1532.80 Å. The presence of these blends can be seen clearly in the spectra of stars with a relatively small terminal velocity where the blue wing of the P Cygni profile reaches the continuum at a wavelength greater 1533 Å, e.g., HD 37043, HD 149038 and HD 37742. The influence of this blend at stars with a higher terminal velocity can be seen in e.g., HD 93250, HD 15558 or HD 101190.

N V 1238.81 and 1242.80 Å

The N V resonance lines are saturated in the range of O3 to B 0 for class I stars. In class III and V stars the N V lines are strong but not saturated. They reach a maximum around O7 for class III stars and O6 for class V stars. The lines are blended with the wing of the interstellar Ly α lines. The correction for this line was described in 3.4, and the fits show that this correction works very well. The resulting estimates of N_H will be discussed in section 7.

We did not obtain a fit of the N V lines for HD 15558, which does not show a clear N V P Cygni profile, and for HD 14947 which has a very noisy spectrum in the wavelength range of the N V lines.

Si IV 1393.76 and 1402.77 Å

The separation of the doublet components by 9 Å produces partly separated P Cygni profiles. Only the stars of luminosity class I show prominent P Cygni profiles. The lines are strongest in stars of type O8 I and decrease in strength towards both the hotter and cooler stars.

C III 1174.92 – 1176 Å

This sextet of lines was treated as a singlet with a central wavelength of 1175.66 Å. This line does not appear in the printed version of the atlas by Walborn *et al.* (1985) but it is present in the version on magnetic tape. Because of the decreasing sensitivity of the IUE satellite in this part of the spectrum many of the spectra are contaminated with noise, which in some cases prevented the fitting of a profile. The fitting of the C III lines is complicated by the presence of a strong photospheric component in many of the spectra. Since we treated the line as a singlet we could only mimic one photospheric line instead of six. This makes the values of A_{phot} but especially w_{phot} rather uncertain.

All the lines with a prominent P Cygni profile turned out to be of class I and III. Thus spectral line is gaining strength from O 4 to later types and is well developed for O 7 and later.

N IV 1718.55 Å

This line has extended violet absorption wings in the spectra of most stars, and shows clear P Cygni profiles in stars of types O 7.5 and earlier. In all cases, however, the line is unsaturated.

The UV morphology described here roughly agrees with those given by Heck *et al.* (1984), Walborn and Panek (1984a, b) and Walborn and Nichols-Bohlin (1987).

4. The terminal and turbulent velocities.

4.1 THE TURBULENT VELOCITY. — This is the first study in which the turbulent velocity in the winds of a large number of stars is estimated. The turbulent velocity has been determined previously for only a few stars, based on detailed studies of individual stars. Lamers and Rogerson (1978) found that the O VI and N V lines of τ Sco indicated a turbulent velocity of 150 km/s in the lower part of the wind. Hamann (1981b) who used the CMF method to analyze τ Sco found a value of 100 km/s in the low velocity layers. Hamann (1980) found for ζ Pup a value of 100 km/s in both the deepest and the outer most layers. The derived turbulent velocities, listed in table I, are in the range of 110 to 370 km/s, with the exception of HD 101413 which has a high but very uncertain value of 580 ± 290 km/s. Groenewegen *et al.* (Paper II) studied the relation between

$v_{\rm turb}$ and $T_{\rm eff}$ and between $v_{\rm turb}/v_\infty$ and $T_{\rm eff}$. They found no clear correlation, except a faint indication that $v_{\rm turb}/v_\infty$ decreases from about 0.15 at O 9 – B 0 I stars to about 0.08 at the early-O stars. This relation, however, may be spurious because the cooler stars are mainly supergiants which have a low value of v_∞, whereas the sample of early-O stars contains supergiants, giants and main sequence stars, which on the average have a higher v_∞. There is no evidence for a relation between $v_{\rm turb}$ and v_∞ nor of a difference in $v_{\rm turb}$ between different luminosity classes. We conclude that the turbulent velocity derived from our line fits does not correlate with spectral type, luminosity class or v_∞.

This lack of correlation may either be due to the simplified manner in which it is treated in our profile calculations or it may be real. If the assumed turbulence is in reality due to random chaotic motions in the wind, the very nature of these random motions might make it impossible to find a correlation between their velocity and the stellar or wind parameters on the basis of snap-shot spectra which will reflect the mean velocity at one moment only.

4.2 THE TERMINAL VELOCITIES. — The implications of the values found for the terminal velocity in this study have been discussed in Paper II. We will summarize the results and conclusions important to this study.

Lamers *et al.* (1987) have demonstrated that the inclusion of turbulence in the calculation of line profiles would produce a shift of the blue absorption edge of saturated lines to shorter wavelengths by about 2 $v_{\rm turb}$. As we have seen in section 4.1 we find turbulent velocities on the order of 100 to 350 km/s. This implies that the terminal velocities derived from the edge velocities of the UV resonance lines are generally overestimated by 200 to 700 km/s. Groenewegen *et al.* found that the values of v_∞, derived from line fitting with the Sobolev-method, are larger than the new values by about 400 km/s. A least squares fit of the relation between the edge velocity of the saturated P Cygni profiles, $v_{\rm edge}$, and our determination of v_∞ shows that

$$v_\infty = (0.87 \pm 0.05)\, v_{\rm edge}. \qquad (17)$$

This implies that our values of v_∞ are systematically about 13% smaller than those derived previously from fitting with Sobolev line profiles. This has immediate consequences for the values of the mass loss rates derived from Hα, infrared, and radio observations for which the inferred mass loss scales with v_∞ as $\dot{M} \sim v_\infty$, and for the mass loss rates derived from UV line fitting for which $\dot{M} \sim v_\infty^2$ (see Sect. 7). So the mass loss rates derived by adopting v_∞ from $v_{\rm edge}$ or from Sobolev profiles are systematically too large by about 15% for $\dot{M}$ from Hα, infrared and radio data and by about 30% for $\dot{M}$ derived from Sobolev fits of UV lines.

5. The slope of the velocity law.

We adopted the velocity law of equation (3) with $w_0 = 0.01$ which was originally proposed by Lamers and Rogerson (1978) and by Castor and Lamers (1979). The values of β, which describes the steepness of the velocity law, are listed in table I. The values of β range from 0.5 to 1.0 with a mean value of $\bar{\beta} = 0.68 \pm 0.15$. The values of β are plotted versus $T_{\rm eff}$ in figure 4. There is no indication of a temperature dependence of β, nor a systematic difference between class V, III or I stars. We will compare our values with other determinations and with predicted values.

In most studies of the UV line profiles published so far the value of β was adopted rather than derived for each star individually. Gathier *et al.* (1981) adopted $w_0 = 0.01$ and $\beta = 1$. Olson and Castor (1981) adopted $w_0 = 0.02$ and $\beta = 0.5$. Garmany *et al.* (1981) adopted $\beta = 0.5$ or $\beta = 1$. Conti and Garmany (1980) adopted $\beta = 1$ for the two stars which they have in common with our sample : HD 93250 and 9 Sgr for which we derived $\beta = 0.7$ and 0.9 respectively. Prinja and Howarth (1986) and Howarth and Prinja (1988) adopted $\beta = 1$.

Bertout *et al.* (1985) investigated the influence of mass loss and the velocity law on the IR-excess from stellar winds. The determination of β was one of their goals. Four of their stars also appear in our sample. These are HD 14947, μ Nor, HD 151804 and λ Cep, for which they found $\beta = 1.5$, 6^{+2}_{-3}, 2.25 and < 1 respectively, whereas our values are $\beta = 0.7$, 0.7, 1.0 and 0.6. Their values are clearly higher than ours. For their total sample they derived $\beta \simeq 1$ for O 4 stars and β increases with spectral type to $\beta \simeq 2$ for B 0 I stars. One should realize that their value of β is determined from the IR-excess and thus reflects the slope of the velocity law in the lower wind layers only. There may be another effect which results in an overestimate of β from IR measurements. Bertout *et al.* adopted plane parallel model atmospheres to subtract the photospheric flux from the observed fluxes and obtained small IR excesses on the order of a few tenths of magnitudes or less. Extension effects in the atmospheres of O-stars and B supergiants will result in a flattening of the photospheric energy distributions in the near-IR (Hummer, 1982). The neglect of these extension effects will result in an overestimate of the near-IR excess and will hence lead to an overestimate of β. This may be the reason for the higher values of β derived by Bertout *et al.* (1985).

Leitherer (1988) studied the strength of the Hα emission in O B stars and combined this with mass loss rates calculated from the mean $\dot{M}(L)$ relation from Garmany and Conti (1984) derived from UV lines. He concludes that $\beta \simeq 0.7$ for O-stars. A close inspection of his figures 2 and 4 shows that β rises from about 0.5 at O 4 to 0.9 at B 0. We did not find such a trend (Fig. 4).

We will now compare our derived values of β with those predicted by the radiation driven wind theory. The original version (Castor *et al.*, 1975) predicted $\beta = 0.5$. Since then the theory has been refined. Friend and Castor (1983) included multiple scattering and found $\beta \simeq 1$. Friend and Abbot (1986) included the important effect of the finite size of the star and found $\beta \simeq 0.8 \pm 0.08$. The same conclusion was reached by Pauldrach *et al.* (1986).

Pauldrach *et al.* (1989) have calculated new non-LTE stellar wind models for a grid of hot stars. A fit of the values of β for these models to the values of the force multipliers α and δ shows that

$$\beta \simeq 1.30\alpha - 0.053\left(v_{\rm esc}/500\ {\rm km\ s^{-1}}\right) - 0.00025/\delta \quad (18)$$

with a mean derivation of $\overline{\Delta\beta} \simeq 0.017$. A functional relation of this type was proposed earlier on the basis of the stellar wind models by Pauldrach *et al.* (1986). The non-LTE calculations show that the force multiplier parameters α and δ are in the range of $0.678 \leq \alpha \leq 0.737$ at $32000 \leq T_{\rm eff} \leq 50000$ K with a mean value of $\bar{\alpha} = 0.695$ and $0.061 \leq \delta \leq 0.087$ at $35500 \leq T_{\rm eff} \leq 50000$ K and $0.028 \leq \delta \leq 0.037$ at $32000 \leq T_{\rm eff} \leq 35500$ K. Using these non-LTE values of α and δ we find the predicted values of β for our program stars are $\bar{\beta}_{\rm pred} = 0.80 \pm 0.03$. This value is higher than the value of $\bar{\beta}_{\rm obs} = 0.68 \pm 0.15$ derived from the observations. There are two possible explanations for this discrepancy : the neglect of limb darkening in the stellar wind models or errors in the predicted radiative forces, i.e., in the force multipliers.

The limb darkening was neglected in the stellar wind models. The inclusion of limb darkening will result in a forward peaking of the stellar radiation which leads to a lower value of β. This effect is quantitatively similar to the neglect of the finite size of the star in the original stellar wind models, which resulted in too steep velocity laws and thus in too small values of β.

The discrepancy between $\bar{\beta}_{\rm obs}$ and $\bar{\beta}_{\rm pred}$ may also be due to an overestimate of the predicted values of α. Groenewegen *et al.* (Paper II) showed that the derived terminal velocities of the winds are smaller than those predicted on the bases of the mentioned values of α and δ. They argued that a decrease of α from 0.695 to $\simeq 0.62$ would match the observed and predicted terminal velocities. If we adopt $\alpha = 0.62$ in equation (18) we predict $\beta_{\rm pred} = 0.70 \pm 0.03$ for our program stars, which agrees very well with the mean value of $\bar{\beta}_{\rm obs} = 0.68 \pm 0.15$ derived from the observations.

We conclude that the value of $\beta_{\rm obs}$ is about 0.68 ± 0.15 in the wind of O-stars and that this agrees with the predicted value of $\beta_{\rm pred} \simeq 0.70$ if $\alpha \simeq 0.62$, which is the value of α suggested by the relation between the observed and predicted terminal velocities. This value of α is smaller than the predicted non-LTE value of $\alpha \simeq 0.695 \pm 0.012$.

6. Comparison with comoving frame and Sobolev fits.

6.1 COMPARISON WITH RESULTS FROM COMOVING FRAME FITS. — The UV lines of the star ζ Pup have been studied with the comoving frame method by Hamann (1980) and Puls (1987). We compare our results in terms of $\dot{M}q_i(v = 0.5\ v_\infty)$, where $\dot{M}$ represents the mass loss in $M_\odot$/yr and q_i the ionization fraction of ion i (see Sect. 7 for details), with those of Hamann at $r = 1.5\ R_*$ where $v = 0.6\ v_\infty$ for his velocity law. We can derive the value of $\dot{M}q_i$ from Puls' publication by combining his published value of $\dot{M} = 4.3 \times 10^{-6}\ M_\odot$/yr with the ionization fractions at $v = 0.5\ v_\infty$ for ζ Pup published by Pauldrach (1987). The results are listed in table VI.

We see that the values of $\dot{M}q_i$ derived from the unsaturated C III and Si IV lines agree very well with the values by Hamann. Our results of C IV and N V agree with the lower limits of $\dot{M}q_i$ derived by Hamann. The values of $\dot{M}q_i$ for the saturated C IV and N V lines by Puls do not contradict our lower limits for $\dot{M}q_i$. Puls did not try to find the best fitting theoretical profile but used a model of the wind of ζ Pup and showed that the resulting profile of N V agreed very well and the C IV profile reasonably well with the observations.

Puls *adopted* a turbulent velocity of 200 km/s for making these profile fits. As we have demonstrated in section 3.7, the choice of the value of $v_{\rm turb}$ has a significant impact on the shape of saturated line profiles. If we would have *adopted* $v_{\rm turb} = 200$ km/s we would have found a value of the optical depth $T_{\rm R}$ for C IV of $T_{\rm R} \approx 65$ ($\pm$30%). This would have resulted in $\log \dot{M}q_{\rm C\ IV} = -7.4 \pm 0.6$, a value close to the one found by Puls. We however did not adopt $v_{\rm turb}$ but fitted this parameter using all lines of each star and found for ζ Pup a value $v_{\rm turb} = 290 \pm 70$ km/s. There is another worrying fact which questions Puls' value of $\dot{M}q$. The values of $\dot{M}q_{\rm C\ III}$ derived from observations by us and by Hamann (1980) agree very well, while the theoretical prediction by Puls differs by a factor of 10^3. This suggests that the ionization balance of carbon derived by Puls tends to higher ionization stages, which is contradicted by the observations. This is partly due to the fact that Puls neglected dielectronic combination.

We conclude that the values of $\dot{M}q$ derived from the observations for all ions agree very well for both SEI and CMF method, and that the theoretical values by Puls are possibly wrong.

6.2 COMPARISON WITH RESULTS FROM SOBOLEV LINE FITS. — In this section we will compare the integrated optical depth derived from our line fits with the SEI-method with those derived from Sobolev line fits.

Gathier *et al.* (1981) used the Copernicus spectra of 25 stars to analyse the lines of C III, N V, O VI, Si III, Si IV, and P V. They adopted the Sobolev profiles calculated by Castor and Lamers (1979) and the corrections for the formation of doublets described in that paper. Their values of the integrated optical depth T for the lines N V, Si IV and C III λ1175 Å will be compared with our results.

Garmany *et al.* (1981) used IUE spectra of 31 O stars to analyze the lines of C IV, N IV, N V and O IV with the grid of profiles calculated by Castor and Lamers (1979). Their values of T for the lines of C IV, N V and N IV will be compared with our results.

Olson and Castor (1981) used the Copernicus observations of the lines of C III λ977 Å, N III, N V, O VI, Si III, Si IV and S IV and the IUE observations of the C IV lines in

eight stars for the analysis of the UV line profiles. They calculated the theoretical profiles in the Sobolev approximation with the escape probability method, properly allowing for the radiative coupling in the formation of the doublets. We will compare their results in terms of T with our results of C IV, N V, and Si IV lines.

Howarth and Prinja (1988) have analyzed the C IV, N V and Si IV lines in the high resolution IUE spectra of 203 galactic O-stars, using the Sobolev profiles calculated with the integral method (Lucy, 1971) and the approximate corrections for doublets from Castor and Lamers (1979). Their values of T are compared with our results.

Figure 5 shows the comparison between our values of T with those from the studies using the Sobolev method. The upper part of figure 5 shows the comparison with different symbols for different authors, whereas the lower part has different symbols for different ions. Figure 5 shows a surprisingly large scatter in T of the order of $\Delta \log T \simeq 0.8$ with extensions up to $\Delta \log T = 1.4$! Figure 5a shows that the large scatter is mainly due to systematic differences between the results of different authors. The values of T derived by Howarth and Prinja (HP) and by Gathier *et al.* (GLS) are systematically lower than ours, those of Garmany *et al.* (G) are systematically higher, while those of Olson and Castor (OC) scatter around our values. We have tried to find an explanation for these distressingly large differences by comparing our profile fits with those obtained by others with the Sobolev method.

Gathier *et al.* (1981) published only a small set of profiles, but the complete set is available to us. Their fits match the observations quite accurately, so one might expect reliable values of T. A comparison between the *observed* profiles used by Gathier *et al.* and ours show that the absorptions in the Copernicus profiles are systematically too weak. This is obviously due to a wrong correction for the background or scattered radiation in the Copernicus spectra. For instance, the Si IV profiles of α Cam (HD 30614), which clearly reach zero intensity in the IUE spectra (see Fig. 2a), reach about 10% in the Copernicus spectra. This results in a difference of $\log T_{\rm red}$(our) = 1.48 and $\log T_{\rm red}$(GLS) = 0.57. Most of the systematic differences between GLS' and our results are due to this effect.

Garmany *et al.* (1981) published only a small fraction of their profile fits. In their analysis of the N V lines they did not correct for the strong absorption due to interstellar Ly α. This means that their values of T(N V) are overestimated. For instance, their analysis of the N V lines of HD 93250 without correction for Ly α yield $\log T_{\rm red}$= 0.70, whereas our analysis which includes a Ly α correction yields $\log T_{\rm red}$= 0.40. For the C IV lines of HD 93250 the derived values of T are very similar.

Olson and Castor (1981) used IUE spectra of the C IV lines and Copernicus spectra of the other lines. The values of T(C IV) derived by OC scatter around our values with a difference of $\Delta \log T \simeq 0.5$. This is due to the fact that C IV lines are often saturated. Since the profiles of saturated lines cannot be reproduced by Sobolev profiles, the choice of the best-fitting calculated profile becomes subjective, which results in a nonsystematic scatter. This effect is clearly seen in the fits of the C IV lines published by OC. The analysis of the other lines, which are generally weaker, is based on Copernicus observations. For the weaker lines OC find higher values of T than our study. An inspection of the profile fits published by OC shows that this is due to the fact that their adopted theoretical profiles are generally stronger than the observed profiles because they tried to take into account the presence of the narrow components (see Fig. 4 by OC). As a result of this, OC's values of T are higher than ours for the weaker lines and smaller than ours for the stronger lines.

Unfortunately, Howarth and Prinja (1988) did not publish their profiles, so the reason for their underestimates of T cannot be checked.

We conclude that a large fraction of the scatter and of the systematic differences between our results and those obtained by others are due to the instrumental effects, to the limitation of the Sobolev method for strong lines, and to the subjective selection of the best theoretical fit in cases when these do not match the observations. Since we used the highest quality UV spectra available up to now and the SEI method which is not hampered by the limitations of the Sobolev approximation, our theoretical profiles in general agree very well with the observations. Therefore our results are expected to be considerably more accurate than those derived earlier.

In a small number of cases the differences between the results obtained by other authors and our results is due to variability of the UV line profiles. For instance the Si IV profiles of ζ Ori observed by the Copernicus satellite, which are used by Olson and Castor and by Gathier *et al.* are very different from those observed with IUE. We expect that this variability of the P Cygni profiles will introduce an error in T in a small number of cases only because in general, the profiles observed with IUE are quite similar to those observed with Copernicus about ten years earlier, if the Copernicus spectra are properly corrected for the scattered light contribution.

In the comparison described above we have compared the integrated optical depths T derived with the Sobolev method and with the SEI method. We also have compared the values of $\tau(v = 0.5\ v_\infty)$ derived by the two methods because various authors have used $\tau(v = 0.5\ v_\infty)$ to derive the mass loss rates of O-stars from UV line profiles. This comparison is not shown here, because the results are similar to those shown in figure 5, i.e., the derivations from the mean relation are about a factor 3 with occasional differences up to a factor 10.

7. The product of mass loss rate and ionization fraction : $\dot{M} q_i$.

The optical depth $\tau(v)$ derived from the line fits can be used to derive the product $\dot{M} q_i$ for each star and each ion i. For the resonance lines, for which $n_u << n_\ell$ (Eq. (4)) the optical depth is

$$\tau(v) = (\pi e^2/mc)\ f\lambda_0\, n_i\, (dv/dr)^{-1} \qquad (19)$$

where n_i is the number density of ion i. This number density can be expressed in the mass loss rate by using the mass continuity equation. This yields

$$n_i = (n_i/n_E)\,(n_E/n_H)\,(n_H/\rho)\,\dot{M}/4\pi r^2 v \qquad (20)$$

where $n_i/n_E = q_i$ is the ionization fraction of ion i of element E, $n_E/n_H = A_E$ is the abundance relative to hydrogen, n_H/ρ is the number of hydrogen atoms per gram which is equal to $(1.4\ m_H)^{-1}$ for a Pop I gas, and $\dot{M}$ is the mass loss rate. Combining equations (19) and (20) and normalizing r and v to R_* and v_∞ yields

$$\dot{M} q_i(w) = 1.189 \times 10^{-18}\, R_* v_\infty^2\ (f\, A_E \lambda_0)^{-1}\, \{\tau(w) x^2 w\ dw/dx\} \qquad (21)$$

with $\dot{M}$ in $M_\odot$/yr, R_* in $R_\odot$, v_∞ in km/s and λ_0 in Å. For nonresonance lines the left hand side of equation (21) should read $\dot{M} q_i(w) E_i(w)$ where E_i is the excitation fraction of the lower level of the observed transition. The adopted abundances are listed in table III. Since the right hand side of equation (21) is known from the line fits we can derive $\dot{M} q_i(w)$ at any point in the wind. The values of $\dot{M} q_i$ for the resonance lines and of $\dot{M} q_i E_i$ for the excited lines are listed in table VII for $w = 0.5$. The errors quoted include all possible errors in T, α_1, α_2, β, v_∞ and R_*. These values will be used in a subsequent paper on a study of the ionization equilibrium in the winds of O-stars.

8. The interstellar H I column densities versus $E(V-B)$.

In section 3.4 we described the correction of the N V line profile for the interstellar Ly α line. The profile fits of N V thus provide an estimate of the values of N_H, i.e., column density of interstellar H I. The values are listed in table VIII together with the values derived by Bohlin *et al.* (1975) from Copernicus observations for the stars in common. The accuracy of our determination of N_H is based on a judgement of the accuracy of the line fits and of the extend of the Ly α wing which is not disturbed by the N V lines.

The agreement between our values of N_H and those of Bohlin *et al.* (1978) is very good and the difference is always in the range of the errors. On the average our values are 10% larger than those of Bohlin *et al.*

The data are plotted in figure 6 in log N_H versus log $E(B-V)$ since $E(B-V) \sim N_H$. The logarithmic mean value of $N_H/E(B-V)$ is

$$\log\{N_H/E(B-V)\} = 21.58 \pm 0.10 \qquad (22)$$

if the stars with $\Delta \log N_H = 0.5$ and the stars with $E(B-V) < 0.10$ are excluded. If these stars are included the mean value is 21.60 ± 0.13. Bohlin *et al.* found a mean of 21.68 ± 0.11 from their study of the Ly α line in the spectra of 100 stars. The difference between our mean value and the one by Bohlin *et al.* is probably due to the fact that their sample of stars covers a wider range in directions than our sample.

9. Summary and discussion.

We have described the results of a study of the UV line profiles from the winds of O-stars with the SEI method. The SEI method eliminates a number of the limitations and problems encountered in the UV line fitting with the Sobolev method. The resulting profile fits (Fig. 2) are considerably more accurate than those obtained in previous studies of the UV line profiles with the Sobolev method.

The accuracy of the line fits enables an accurate determination of the velocity laws of the winds of O-stars. The terminal velocities are smaller than derived from studies of the line profiles with the Sobolev method by about 13%, because the terminal velocities of the winds are smaller than the edge velocities of the strong UV lines. Groenewegen *et al.* (1988) have shown that the derived values of v_∞ are smaller than those predicted by the radiation driven wind theory if the stellar parameters are derived from evolutionary tracks.

The slope of the velocity law, which is characterized by the value of β (Eq. (3)) is $\bar{\beta} = 0.68 \pm 0.15$ (Sect 5). This is slightly lower than the value of $\beta = 0.80$ predicted for our stars from the radiation driven wind theory. If the value of the force multiplier α in the wind theory were $\alpha \approx 0.62$ as suggested in Paper II instead of the predicted value of 0.695 (Pauldrach *et al.*, 1989), the predicted terminal velocity and the predicted value of β would agree with the observations.

The results of our line fits in terms of the integrated optical depth T, which is proportional to the column densities of the observed ions, are compared with those derived from line fits with the Sobolev method by Gathier *et al.* (1981), Garmany *et al.* (1981), Olson and Castor (1981) and Howarth and Prinja (1988) in Section 6. These differences are surprisingly large and range from typical factors of 3 to as much as 10. There are larger systematic differences between the results of the analysis of the *same* stars by different authors if the Sobolev method is used. This is due to the fact that the predicted Sobolev profiles do not match the observed profiles accurately enough. As a result, the choice of the best fit theoretical profile becomes arbitrary and subjective. On the average Gathier *et al.* (1981) and Howarth and Prinja (1988) tend to underestimate the optical depths of the lines by about a factor 2 to 3. Garmany *et al.* (1981) tend to overestimate the optical depth by about a factor 2, whereas Olson and Castor

(1981) overestimate the optical depths slightly. Apart from these general trends there are large differences between the SEI results and the Sobolev results from star to star and from ion to ion. These differences are particularly large when the lines are very strong and approach saturation. In those cases the Sobolev profiles do not resemble the observed profiles and they give very little information on the variation of $\tau(v)$.

The large differences between the Sobolev and SEI results are discouraging. When we started this project we hoped that the results from the SEI method would differ from the Sobolev results in a systematic and predictable way. This would allow the possibility of using the Sobolev results by applying a well defined correction factor. The large random differences however, demonstrated in figure 5, show that such a simple correction is not possible and that the results of the Sobolev fits should be considered doubtful. This has important consequences : (i) Most of the information about the mass loss from hot stars is derived from the UV lines. If the optical depths and column densities are uncertain by a factor 3 to 10, then the mass loss rates are uncertain by about the same factor. (ii) An essential step in the determinations of the mass loss from the UV lines is the correction for the ionization fraction q_i ((Eq. (21)). In most studies the ionizaton fractions are calculated or estimated on the basis of the observed ionization ratios of different ions, e.g. $q(\mathrm{C\ IV})/q(\mathrm{N\ V})$, which provides information on the ionization balance in the wind. If the optical depths or the column densities derived from the UV lines are uncertain by a factor 3 to 10, the ionization ratios will also be uncertain and consequently the adopted ionization fractions may be wrong. This introduces an additional uncertainty in the derived mass loss rates.

The ionization in the stellar winds will be studied in a forthcoming paper, based on the results of the study presented here.

Acknowledgements.

We thank the Astronomical Data Center of NASA Goddard Space Flight Center for providing us with the magnetic tape of the IUE atlas of Walborn *et al.* (1985) which was essential for this study. The second author is grateful to P. Conti, C. Garmany and T. Snow for hospitality at JILA and CASA (Boulder) in the summer of 1988 where part of this study was carried out. We thank the staff of the JILA Scientific Reports Office for preparing the manuscript. This research was supported in part by National Science Foundation grant AST88-06594, by NASA grant NSG-5300 to the University of Colorado.

Appendix I. The effect of limb darkening on the SEI method.

We will describe in this appendix what mathematical changes are needed to the original SEI method to incorporate limb darkening. At three places the formulae given by Lamers *et al.* (1987) should be changed :
1) β_{cB} and β_{cR} (their Eqs. (6) and (23)) : under the integral sign there should be a term $[1 - a(1-\mu) - b(1-\mu)^2]$.
2) $I_\nu(p)$ for $p < 1$ (their Eq. (15)) : I_ν^* should be replaced by Eq. (19).
3) F_ν (their Eq. (19)) : F_ν should be divided by

$$F_{\mathrm{c}} = 2 \int_0^1 \mu \left[1 - a(1-\mu) - b(1-\mu)^2 \right] \mathrm{d}\mu \qquad \text{(A1)}$$

One should be careful about the following. For some μ, $I(\mu)$ may become negative. This is because a and b have no physical meaning but are only mathematically derived fit parameters. In those cases we set $I(\mu) = 0$. This is the reason why we have not explicitly calculated F_{c}(Eq. (A1)) in terms of a and b. The integral should be evaluated only for a positive integrand.

References

BERTOUT C., LEITHERER C., STAHL O., WOLF B. : 1985, *Astron. Astrophys.* **144**, 87.
BOHLIN R. C. : 1973, *Astrophys. J.* **182**, 139.
BOHLIN R. C., SAVAGE B. D., DRAKE J. F. : 1978, *Astrophys. J.* **224**, 132.
CASTOR J. I. : 1970, *Mon. Not. R. Astron. Soc.* **149**, 111.
CASTOR J. I., LAMERS H. J. G. L. M. : *Astrophys. J. Suppl. Ser.* **39**, 481.
CHLEBOWSKI T., GARMANY C. D. : 1988, in preparation.
CONTI P. S., GARMANY C. D. : 1980, *Astrophys. J.* **238**, 190.
FRIEND D. B., ABBOT D. C. : 1986, *Astrophys. J.* **311**, 701.
FRIEND D. B., CASTOR J. I. : 1983, *Astrophys. J.* **272**, 259.
GARMANY C. D. : 1987, private communication.
GARMANY C. D., CONTI P. S. : 1984, *Astrophys. J.* **284**, 705.
GARMANY C. D., OLSON G. L., CONTI P. S., VAN STEENBERG M. E. : 1981, *Astrophys. J.* **250**, 660.
GATHIER R., LAMERS H. J. G. L. M., SNOW T. P. : 1981, *Astrophys. J.* **247**, 173.
GROENEWEGEN M. A. T., LAMERS H. J. G. L. M. : 1989, *Astron. Astrophys.* (in preparation) Paper III.
GROENEWEGEN M. A. T., LAMERS H. J. G. L. M., PAULDRACH A. W. A. : 1989, *Astron. Astrophys.* (in press), Paper II.
HAMANN W. -R. : 1980, *Astron. Astrophys.* **84**, 342.
HAMANN W. -R. : 1981a, *Astron. Astrophys.* **93**, 353.
HAMANN W. -R. : 1981b, *Astron. Astrophys.* **100**, 169.
HECK A., EGRET D., JASCHEK M., JASCHEK C. : 1984, IUE Low Resolution Spectral Atlas : Part 1. Normal Stars, ESA-SP 1052.

HENRICHS H. F. : 1988, in O stars and Wolf Rayet Stars, P. S. Conti and A. B. Underhill Eds. (NASA SP-497) p. 199.
HOWARTH I., PRINJA R. K. : 1989, *Astrophys. J. Suppl. Ser.* **69**, 527.
HUMMER D. G. : 1982, *Astrophys. J.* **257**, 724.
JENKINS E. B. : 1971, *Astrophys. J.* **169**, 25.
KURUCZ R. L. : 1979, *Astrophys. J. Suppl. Ser.* **40**, 1.
LAMERS H. J. G. L. M. : 1988, in Mass Outflows from Stars and Galactic Nuclei, L. Bianci and R. Gilmozzi Eds. (Reidel, Dortrecht) p. 39.
LAMERS H. J. G. L. M., MORTON D. C. : 1976, *Astrophys. J. Suppl. Ser.* **32**, 715.
LAMERS H. J. G. L. M., ROGERSON J. B. : 1978, *Astron. Astrophys.* **66**, 417.
LAMERS H. J. G. L. M., GATHIER R., SNOW T. P. : 1982, *Astrophys. J.* **258**, 186.
LAMERS H. J. G. L. M., CERRUTI-SOLA M., PERINOTTO M. : 1987, *Astrophys. J.* **314**, 726.
LEITHERER C. : 1988, *Astrophys. J.* **326**, 356.
LUCY L. B. : 1971, *Astrophys. J.* **163**, 95.
LUCY L. B. : 1984, *Astron. Astrophys.* **140**, 210.
MAEDER A., MEYNET G. : 1987, *Astron. Astrophys.* **182**, 243.
MIHALAS D., KUNASZ P. B., HUMMER D. G. : 1975, *Astrophys. J.* **202**, 465.
OLSON G. L., CASTOR J. I. : 1981, *Astrophys. J.* **244**, 179.
PAULDRACH A. W. A. : 1987, *Astron. Astrophys.* **183**, 295.
PAULDRACH A. W. A., PULS J., KUDRITZKI R. P. : 1986, *Astron. Astrophys.* **164**, 86.
PAULDRACH A. W. A., KUDRITZKI R. P., PULS J., BUTLER K. : 1989, *Astron. Astrophys.* (in press).
PRINJA R. K., HOWARTH I. D. : 1986, *Astrophys. J. Suppl. Ser.* **61**, 357.
PULS J. : 1987, *Astron. Astrophys.* **184**, 227.
RYBICKI G. R., LIGHTMAN A. P. : 1979, Radiative Processes in Astrophysics (Wiley, New York).
SCHMIDT-KALER T : 1982, Landolt-Börnstein, New Series, Group VI, Vol 2b, K. Schaifers and H. H. Voigt Eds. (Springer-Verlag, Berlin).
SNOW T. P. : 1977, *Astrophys. J.* **217**, 760.
SNOW T. P., MORTON D. C. : 1976, *Astrophys. J. Suppl. Ser.* **32**, 429.
SOBOLEV V. V. : 1958, Theoretical Astrophysics, V. A. Ambartsumian Ed. (Pergamon Press, New York).
WADE R. A., RUCINSKI S. M. : 1985, *Astron. Astrophys. Suppl. Ser.* **60**, 471.
WALBORN N. R., PANEK R. : 1984a, *Astrophys. J. Lett.* **280**, L27.
WALBORN N. R., PANEK R. : 1984b, *Astrophys. J.* **286**, 718.
WALBORN N. R., NICHOLS-BOHLIN J., PANEK R. : 1985, International Ultraviolet Explorer Atlas of O type spectra from 1200 to 1900 Å (NASA Conf. Publ. 1155).
WALBORN N. R., NICHOLS-BOHLIN J. : 1987, *Publ. Astron. Soc. Pac.* **99**, 40.

TABLE I. — *The program stars.*

HD	Name	Type	IUE SWPnr	E(B-V) (magn)	log T_{eff} (K)	log L ($L_\odot$)	log R ($R_\odot$)	log M ($M_\odot$)	log g (cm/s^2)	v_{esc} (km/s)	v_∞ (km/s)	β	v_{turb} (km/s)
14947		05 I f+	10724	0.76	4.605	5.85	1.24	1.74	3.70	890	2300± 70	0.7±0.1	230±100
15558		05 III (f)	8322	0.84	4.626	6.03	1.29	1.85	3.71	910	3350±200	0.7±0.1	110± 90
15629		05 V ((f))	10754	0.75	4.646	5.72	1.09	1.72	3.98	1090	2900± 70	0.7±0.1	150± 80
24912	ξ Per	07.5III(n)((f))	3040	0.35	4.569	5.32	1.04	1.50	3.86	950	2400±100	0.5±0.15	290±120
30614	α Cam	09.5 Ia	2591	0.28	4.490	5.95	1.52	1.71	3.11	560	1550± 60	0.7±0.1	190± 60
36861	λ Ori	08 III ((f))	10611	0.12	4.556	5.36	1.09	1.51	3.77	900	2400±150	0.5±0.1	290± 70
37043	ι Ori	09 III	11164	0.06	4.532	5.58	1.25	1.59	3.53	790	2450±150	0.6±0.1	370± 70
37128	ε Ori	BO Ia	6726	0.06	4.447	5.80	1.53	1.62	3.00	630	1500±150	0.7±0.1	230± 80
37742	ζ Ori	09.7 Ib	2481	0.04	4.484	5.74	1.42	1.61	3.21	620	2100±150	0.7±0.1	320±130
46150		05 V ((f))	10758	0.46	4.646	5.72	1.09	1.72	3.98	1090	2900±200	0.7±0.1	200± 90
46223		04 V ((f))	10757	0.55	4.667	5.70	1.04	1.73	4.09	1190	2800± 60	0.6±0.1	200± 90
47839	15 Mon	07 V ((f))	13490	0.07	4.603	5.29	0.96	1.54	4.06	1110	2300±200	0.5±0.1	320±110
66811	ζ Pup	04 I (n) f	15629	0.03	4.627	5.87	1.20	1.77	3.81	970	2200± 60	0.7±0.1	290± 70
93129A		03 I f*	14007	0.55	4.648	6.13	1.29	1.92	3.78	960	3050± 60	0.9±0.1	180± 80
93204		05 V ((f))	7023	0.43	4.646	5.48	0.97	1.62	4.12	1170	2800± 60	0.5±0.1	360± 80
93250		03 V ((f))	14747	0.48	4.686	6.08	1.19	1.92	3.98	1120	3300±200	0.7±0.1	260± 80
101190		06 V ((f))	6973	0.39	4.625	5.74	1.14	1.71	3.87	1010	2900±150	0.8±0.1	170± 80
101413		08 V	6971	0.40	4.580	5.23	1.12	1.48	3.68	860	2900±200	0.6±0.1	580±290
101436		06.5 V	6938	0.39	4.615	5.60	1.09	1.64	3.90	1010	2800±150	0.5±0.25	220± 80
149038	μ Nor	09.7 Iab	17396	0.33	4.484	5.70	1.40	1.58	3.22	610	1750±100	0.7±0.1	260±150
151804		08 Iaf	5140	0.36	4.532	6.14	1.53	1.84	3.22	600	1600± 70	1.0±0.1	240± 80
163758		06.5 Iaf	2892	0.34	4.571	5.96	1.36	1.77	3.49	760	2200± 70	0.5±0.1	260±140
164794	9 Sgr	04 V ((f))	6040	0.36	4.667	6.02	1.20	1.87	3.91	1060	2950±150	0.9±0.1	210± 60
188001	9 Sge	07.5 Iaf	3465	0.32	4.545	5.90	1.38	1.72	3.40	710	1800± 70	1.2±0.2	250± 90
190429A		04 I f+	4903	0.47	4.627	6.03	1.28	1.85	3.73	920	2300± 70	0.9±0.1	370±140
190864		06.5 III (f)	10851	0.52	4.593	5.62	1.15	1.62	3.76	910	2450±150	0.5±0.15	125±100
210839	λ Cep	06 I nfp	14938	0.56	4.582	5.87	1.29	1.75	3.61	850	2100± 60	0.6±0.1	210± 70
Typical uncertainties: (dex)					0.02	0.20	0.14	0.10	0.2	0.15			

TABLE II. — *Limb darkening coefficients.*

HD	a_1	b_1	a_2	b_2	HD	a_1	b_1	a_2	b_2	HD	a_1	b_1	a_2	b_2
14947	.32	.23	.26	.26	46150	.29	.25	.24	.27	101436	.31	.25	.25	.27
15558	.31	.22	.25	.26	46223	.28	.25	.23	.27	149038	.39	.22	.38	.21
15629	.29	.25	.24	.27	47839	.30	.26	.24	.28	151804	.30	.26	.33	.22
24912	.33	.25	.26	.28	66811	.31	.23	.25	.26	163758	.36	.21	.30	.25
30614	.37	.23	.38	.20	93129A	.29	.23	.24	.26	164794	.28	.24	.23	.26
36861	.35	.24	.27	.28	93204	.29	.26	.23	.27	188001	.35	.23	.32	.24
37043	.36	.21	.30	.25	93250	.28	.24	.23	.26	190429A	.31	.22	.25	.26
37128	.46	.17	.44	.18	101190	.31	.24	.24	.27	190864	.33	.24	.26	.27
37742	.39	.22	.38	.21	101413	.34	.23	.27	.27	210839	.34	.22	.28	.26

$a_1 = a(1361\ \text{Å}), b_1 = b(1362\ \text{Å}), a_2 = a(1815\ \text{Å}), b_2 = b(1815\ \text{Å})$; typical uncertainty 0.03.

TABLE III. — *The lines studied.*

Ion	λ_0 (Å)	f	g_ℓ	g_u	χ_{exc} (eV)	N_E/N_H
C IV	1548.19	0.194	2	--	0	$3.2\ 10^{-4}$
	1550.76	0.097	2	--		
N V	1238.81	0.152	2	--	0	$7.9\ 10^{-5}$
	1242.80	0.076	2	--		
Si IV	1393.76	0.528	2	--	0	$4.0\ 10^{-5}$
	1402.77	0.262	2	--		
C III	1175.66[a]	0.257	1	9	6.50	$3.2\ 10^{-4}$
N IV	1718.55	0.179	1	3	16.21	$7.9\ 10^{-5}$

a) Six lines at $1174.92 \leq \lambda \leq 1176.35$ Å, treated as one line with the total f-value.

TABLE IVa. — *The parameters of the line fits.*

HD	C IV			N V			Si IV		
	log T_{red}	α_1	α_2	log T_{red}	α_1	α_2	log T_{red}	α_1	α_2
14947	>0.64	2.0±0.5	0.3±0.2	--	--	--	0.96±010	1.0±0.5	1.0±0.2
15558	>1.00	1.8±0.6	4.4±0.6	--	--	--	--	--	--
15629	>0.83	0.0±0.1	0.6±0.1	1.00±0.30	-0.9±0.2	-0.5±0.2	--	--	--
24912	>1.00	0.9±0.3	1.5±0.4	1.06±0.10	4.9±1.0	4.1±0.5	--	--	--
30614	>0.78	0.9±0.1	0.2±0.2	0.69±0.10	-0.3±0.2	-0.3±0.4	>1.18	1.4±0.5	1.0±0.2
36861	1.46±0.10	1.5±0.2	3.1±0.5	0.00±0.10	0.5±0.1	0.4±0.3	--	--	--
37043	0.18±0.10	1.5±0.3	2.0±0.5	-0.10±0.10	0.0±0.1	0.8±0.1	--	--	--
37128	>1.08	4.0±0.5	2.5±0.1	-0.35±0.10	0.7±0.2	0.2±0.1	1.26±0.20	0.6±0.1	4.5±0.2
37742	1.23±0.10	1.4±0.2	2.6±0.6	-0.21±0.10	1.2±0.2	1.2±0.1	0.90±0.10	3.5±0.2	3.7±0.3
46150	0.26±0.10	-1.2±0.1	-0.6±0.1	0.48±0.10	-1.0±0.1	-0.1±0.1	--	--	--
46223	>0.40	0.4±0.2	-0.3±0.1	>0.74	-0.4±0.2	-0.2±0.1	--	--	--
47839	-0.18±0.10	-0.1±0.2	0.3±0.1	0.15±0.10	-1.1±0.1	0.1±0.1	--	--	--
66811	>0.82	1.0±0.3	-0.4±0.1	>0.60	1.0±0.1	-0.1±0.1	-0.04±0.10	0.3±0.2	-0.1±0.1
93129A	>0.48	-1.6±0.5	-1.1±0.3	>0.70	0.0±0.3	1.0±0.3	--	--	--
93204	>0.60	0.0±0.1	0.5±0.1	1.06±0.10	2.9±0.5	4.4±0.5	--	--	--
93250	0.30±0.10	-1.0±0.2	0.0±0.2	0.40±0.20	-0.9±0.2	0.2±0.2	--	--	--
101190	0.34±0.15	-1.0±0.1	-0.4±0.2	0.70±0.10	-1.0±0.2	0.3±0.2	--	--	--
101413	-0.10±0.10	0.8±0.5	1.6±0.4	0.08±0.10	-1.0±0.2	0.3±0.2	--	--	--
101436	0.76±0.10	-0.8±0.3	-0.2±0.2	0.60±0.10	-0.2±0.2	2.0±0.5	--	--	--
149038	>1.08	-0.1±0.2	0.3±0.2	-0.28±0.10	1.9±0.1	0.4±0.5	0.26±0.10	-0.7±0.2	-0.4±0.2
151804	>0.60	0.5±0.3	0.7±0.2	>1.18	0.8±0.1	1.1±0.2	>1.15	3.0±0.5	1.5±0.5
163758	>0.95	2.4±0.5	0.5±0.1	>1.15	1.0±0.1	0.2±0.1	>0.95	4.2±0.5	0.7±0.2
164794	0.90±0.10	-0.1±0.1	0.6±0.1	0.70±0.20	0.3±0.1	1.1±0.2	--	--	--
188001	>0.70	1.0±0.2	1.0±0.2	>0.85	0.3±0.2	0.1±0.1	>1.40	1.0±0.5	2.0±1.0
190429A	0.36±0.10	1.0±0.1	0.6±0.2	0.91±0.20	-0.1±0.2	0.4±0.4	-0.18±0.10	0.5±0.6	-0.4±0.2
190864	>0.66	0.1±0.3	-0.2±0.1	0.46±0.10	1.0±0.5	0.9±0.1	--	--	--
210839	>0.60	1.0±0.3	-0.3±0.2	>0.44	0.4±0.2	-0.5±0.2	0.60±0.10	-0.9±0.1	-0.5±0.1

TABLE IVb. — *The parameters of the line fits.*

HD	C III				N IV			
	log T	α_1	α_2	w_1	log T	α_1	α_2	w_1
14947	--	--	--	--	--	--	--	--
15558	--	--	--	--	-0.10±0.10	-1.0±0.1	2.0±0.5	1.0
15629	--	--	--	--	-0.59±0.10	-0.2±0.1	2.0±0.1	1.0
24912	0.11±0.10	0.2±0.1	0.8±0.1	0.9	-0.48±0.10	-0.5±0.1	1.0±0.2	1.0
30614	>0.30	2.6±0.3	0.6±0.3	1.0	--	--	--	--
36861	0.00±0.10	-0.9±0.2	0.2±0.1	1.0	--	--	--	--
37043	-0.62±0.10	-0.2±0.1	1.6±0.2	1.0	--	--	--	--
37128	0.78±0.10	2.0±0.5	4.0±0.5	1.0	--	--	--	--
37742	1.00±0.10	0.5±0.1	1.6±0.1	1.0	--	--	--	--
46150	--	--	--	--	-0.77±0.10	-0.5±0.1	1.0±0.1	0.6
46223	--	--	--	--	-0.22±0.10	-0.5±0.2	1.2±0.2	0.7
47839	--	--	--	--	--	--	--	--
66811	0.00±0.10	0.0±0.1	0.4±0.1	1.0	0.36±0.10	0.4±0.1	3.5±0.4	1.0
93129A	--	--	--	--	0.18±0.10	-0.8±0.1	0.4±0.1	1.0
93204	--	--	--	--	--	--	--	--
93250	--	--	--	--	-0.35±0.10	-0.5±0.1	1.0±0.1	0.85
101190	--	--	--	--	-0.40±0.10	-0.5±0.1	1.1±0.1	0.80
101413	--	--	--	--	--	--	--	--
101436	--	--	--	--	-0.80±0.20	0.0±0.2	0.5±0.1	0.65
149038	0.00±0.10	1.8±0.1	2.1±0.1	1.0	--	--	--	--
151804	0.48±0.20	0.0±0.5	0.5±0.1	1.0	--	--	--	--
163758	0.62±0.10	1.4±0.2	0.1±0.1	1.0	0.90±0.20	-0.7±0.2	4.0±1.0	0.80
164794	--	--	--	--	-0.46±0.10	-0.5±0.1	2.0±0.2	1.0
188001	0.46±0.10	0.8±0.1	0.5±0.1	1.0	--	--	--	--
190429A	--	--	--	--	0.15±0.10	0.3±0.2	3.0±0.5	1.0
190864	--	--	--	--	-0.15±0.10	-1.0±0.1	0.7±0.3	0.61
210839	0.18±0.10	0.0±0.5	0.3±0.1	1.0	0.60±0.20	-0.5±0.2	4.0±1.0	1.0

TABLE V. — *The adopted photospheric components.*

HD	C IV		N IV		Si IV		C III		N IV	
	A^R_{phot}	w_{phot}	A^R_{phot}	w_{phot}	A^R_{phot}	w_{phot}	A_{phot}	w_{phot}	A_{phot}	w_{phot}
14947	1.8	0.04	--	--	0.0	--	--	--	--	--
15629	0.5	0.05	0.0	--	--	--	--	--	1.2	0.06
24912	0.0	--	0.0	--	--	--	3.0	0.08	0.9	0.04
30614	0.0	--	0.0	--	0.0	--	3.0	0.15	--	--
36861	1.0	0.12	0.4	0.10	--	--	6.0	0.07	--	--
37043	1.0	0.15	0.4	0.08	--	--	3.5	0.09	--	--
37128	0.9	0.10	0.0	--	1.0	0.10	4.0	0.15	--	--
37742	0.7	0.10	1.0	0.03	0.9	0.10	2.0	0.15	--	--
46150	1.0	0.07	1.0	0.03	--	--	--	--	0.8	0.04
46223	0.0	--	1.0	0.07	--	--	--	--	0.7	0.04
47839	0.6	0.12	0.3	0.12	--	--	--	--	--	--
66811	0.0	--	0.7	0.10	1.0	0.10	2.0	0.06	0.0	--
93129A	0.0	--	1.0	0.05	--	--	--	--	0.0	--
93250	0.0	--	3.0	0.05	--	--	--	--	3.0	0.03
101190	1.0	0.05	1.0	0.05	--	--	--	--	1.0	0.04
101413	0.2	0.15	0.3	0.15	--	--	--	--	--	--
101436	1.0	0.03	0.0	--	--	--	--	--	1.1	0.05
149038	1.0	0.05	0.0	--	1.0	0.10	2.0	0.15	--	--
163758	0.0	--	1.0	0.05	0.0	--	0.0	--	0.0	--
164794	1.0	0.05	1.0	0.05	--	--	--	--	1.9	0.04
188001	0.0	--	0.4	0.05	0.0	--	4.0	0.08	--	--
190864	1.0	0.06	1.0	0.06	1.0	0.12	--	--	1.2	0.06
210839	0.0	--	1.0	0.10	0.0	--	2.0	0.08	0.0	--

A_{phot} = 0.0 means : no photospheric component was adopted.
A_{phot} = -- means : no fit of the P Cygni profile.

TABLE VI. — *A comparison of observed and predicted values of* $\log \dot{M} q$ $(v = 0.5\, v_\infty)$ *for* ζ *Pup.*

	SEI-method	Comoving frame method	Predicted
	This work	Hamann (1980)	Puls (1986)
C IV	>-8.38	>-8.17	-7.27
N V	>-7.66	>-7.45	-5.46
Si IV	-8.56±0.10	-8.58±0.15	--
C III	-8.31±0.12[a)]	-8.51±0.30	-11.87

a) Using the observed value of the excitation fraction of the C III 1175 Å transition of 0.1 (Lamers and Morton, 1976).

TABLE VII. — *The products $\dot{M} q_i$ and $\dot{M} q_i E_i$ at $v = 0.5\, v_\infty$* ([a]).

Star HD	log $\dot{M}q_i$ C IV	log $\dot{M}q_i$ N V	log $\dot{M}q_i$ Si IV	log $\dot{M}q_iE_i$ C III	log $\dot{M}q_iE_i$ N IV
14947	>-8.33	--	-7.32±0.23	--	--
15558	>-7.36	--	--	--	-9.05±0.17
15629	>-8.96	-7.41±0.40	--	--	-9.31±0.18
24912	>-7.90	-6.90±0.41	--	-9.26±0.12	-9.49±0.12
30614	>-8.29	-7.62±0.18	>-7.16	>-9.02	--
36861	-7.30±0.19	-8.12±0.15	--	-9.64±0.15	--
37043	-8.46±0.21	-8.13±0.12	--	-9.88±0.14	--
37128	-7.71±0.29	-8.52±0.14	-7.34±0.21	-8.29±0.30	--
37742	-7.39±0.23	-8.03±0.15	-7.07±0.22	-8.04±0.13	--
46150	-9.13±0.13	-7.99±0.13	--	--	-10.16±0.12
46223	>-8.63	>-7.52	--	--	-9.46±0.17
47839	-9.37±0.14	-8.71±0.16	--	--	--
66811	>-8.38	>-7.66	-8.56±10	-9.31±0.12	-8.40±0.13
93129A	>-8.93	>-7.14	--	--	-8.50±0.12
93204	>-8.69	-6.79±0.31	--	--	--
93250	-8.77±0.19	-7.84±0.17	--	--	-9.03±0.12
101190	-8.86±0.14	-7.77±0.18	--	--	-9.34±0.13
101413	-8.79±0.25	-8.39±0.18	--	--	--
101436	-8.42±0.22	-7.54±0.19	--	--	-9.69±0.17
149038	>-7.95	-8.49±0.21	-8.47±0.16	-9.07±0.16	--
151804	>-8.25	>-6.83	>-7.10	-8.76±0.27	--
163758	>-8.93	>-6.84	>-7.62	-8.55±0.20	-8.64±0.24
164794	-7.87±0.13	-7.20±0.19	--	--	-9.30±0.13
188001	>-8.11	>-7.29	>-6.92	-8.77±0.12	--
190429A	-8.42±0.16	-7.14±0.30	-8.57±0.28	--	-8.60±0.24
190864	>-8.35	-7.54±0.23	--	--	-9.84±0.21
210839	>-8.49	>-7.90	-8.18±0.13	-9.08±0.23	-8.58±0.20

([a]) E_i represents the excitation fraction.

TABLE VIII. — *Interstellar N_H versus $E(B-V)$.*

HD	E(B-V)	log N_H [a]	log N_H [b]	HD	E(B-V)	log N_H [a]	log N_H [b]
15629	0.75	21.0±0.5	--	93250	0.48	21.3±0.5	--
24912	0.35	21.08±0.05	21.11±0.07	101190	0.39	21.23±0.10	--
30614	0.28	21.04±0.05	20.90±0.08	101413	0.40	21.1±0.2	--
36861	0.12	20.78±0.05	20.78±0.10	101436	0.39	21.23±0.05	--
37043	0.06	20.18±0.10	20.15±0.06	149038	0.33	21.15±0.05	21.00±0.08
37128	0.06	20.48±0.10	20.45±0.08	151804	0.36	21.15±0.10	21.08±0.12
37742	0.04	20.56±0.10	20.41±0.08	163758	0.34	21.15±0.10	--
46150	0.46	21.32±0.10	--	164794	0.36	21.23±0.10	--
46223	0.55	21.2±0.3	--	188001	0.32	21.11±0.05	21.04±0.11
47839	0.07	20.40±0.05	--	190429A	0.47	21.15±0.20	--
93129A	0.55	21.1±0.5	--	190864	0.52	21.30±0.20	--
93204	0.43	21.32±0.10	--	210839	0.56	21.08±0.10	21.11±0.08

a) Our value.
b) Bohlin *et al.* (1978).

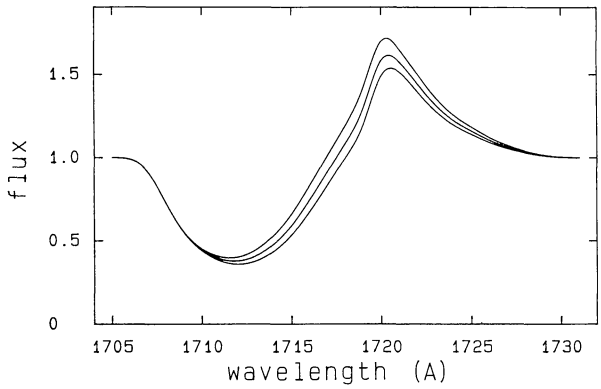

FIGURE 1. — The effect of photospheric limb darkening on the predicted P Cygni profile of an unsaturated N IV λ 1718 line is shown. The predicted profiles are calculated with the following parameters : $T = 2$, $\alpha_1 = \alpha_2 = 0$, $\beta = 0.75$, $v_\infty = 2000$ km/s, $v_{\rm turb} = 200$ km/s. The limb darkening coefficients of the three profiles are from top to bottom : (a, b) =(0.5, 0.5), (0.3, 0.2) and (0, 0). Increased limb darkening increases the flux over a substancial part of the profile.

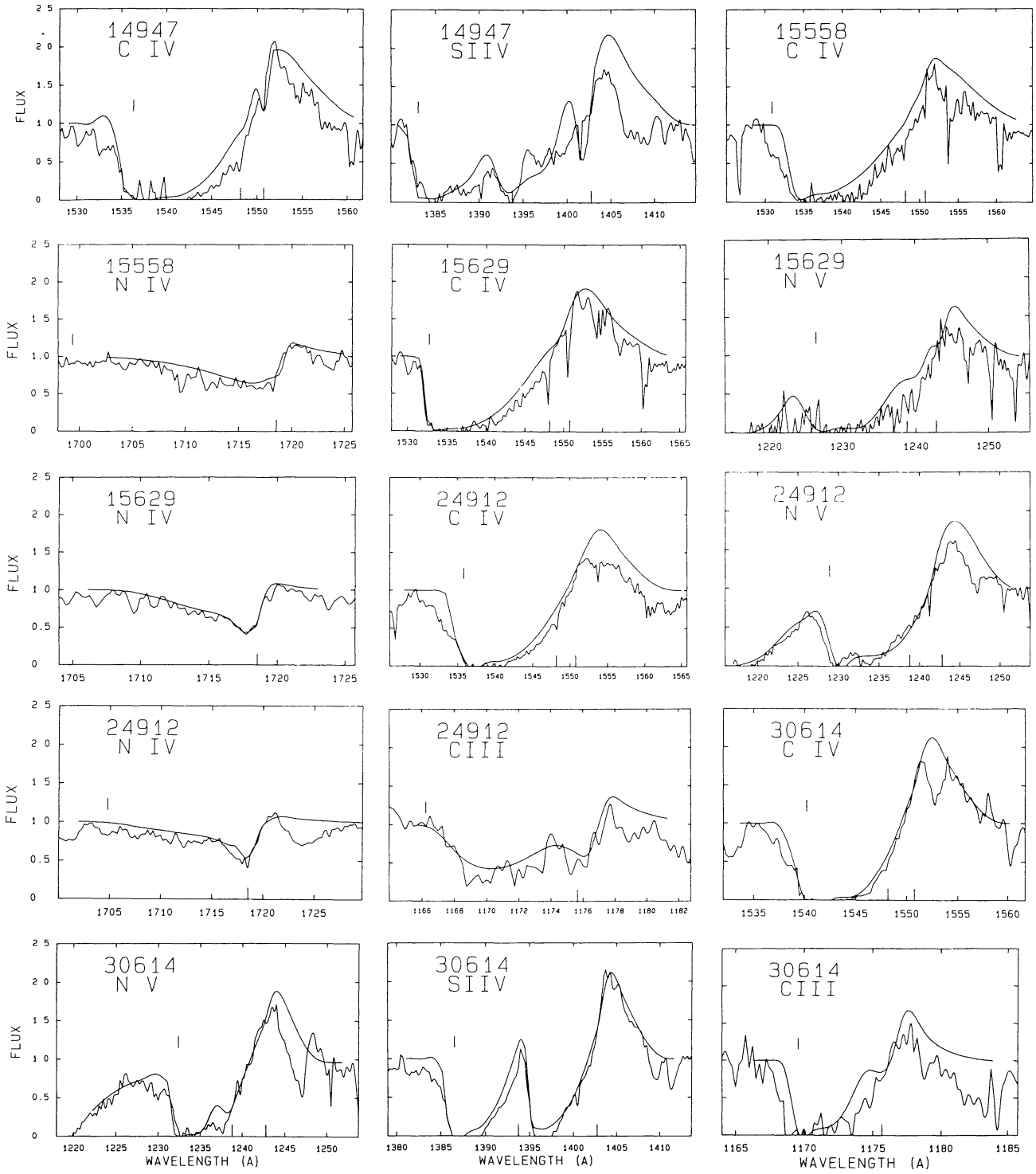

FIGURE 2. — The observed profiles of the UV lines studied in this paper. The adopted line fits are shown by smooth curves. The wavelength corresponding to the terminal velocity is shown by a vertical mark at flux $\simeq$ 1.2. Notice the very good agreement between the observed and calculated profiles in most cases.

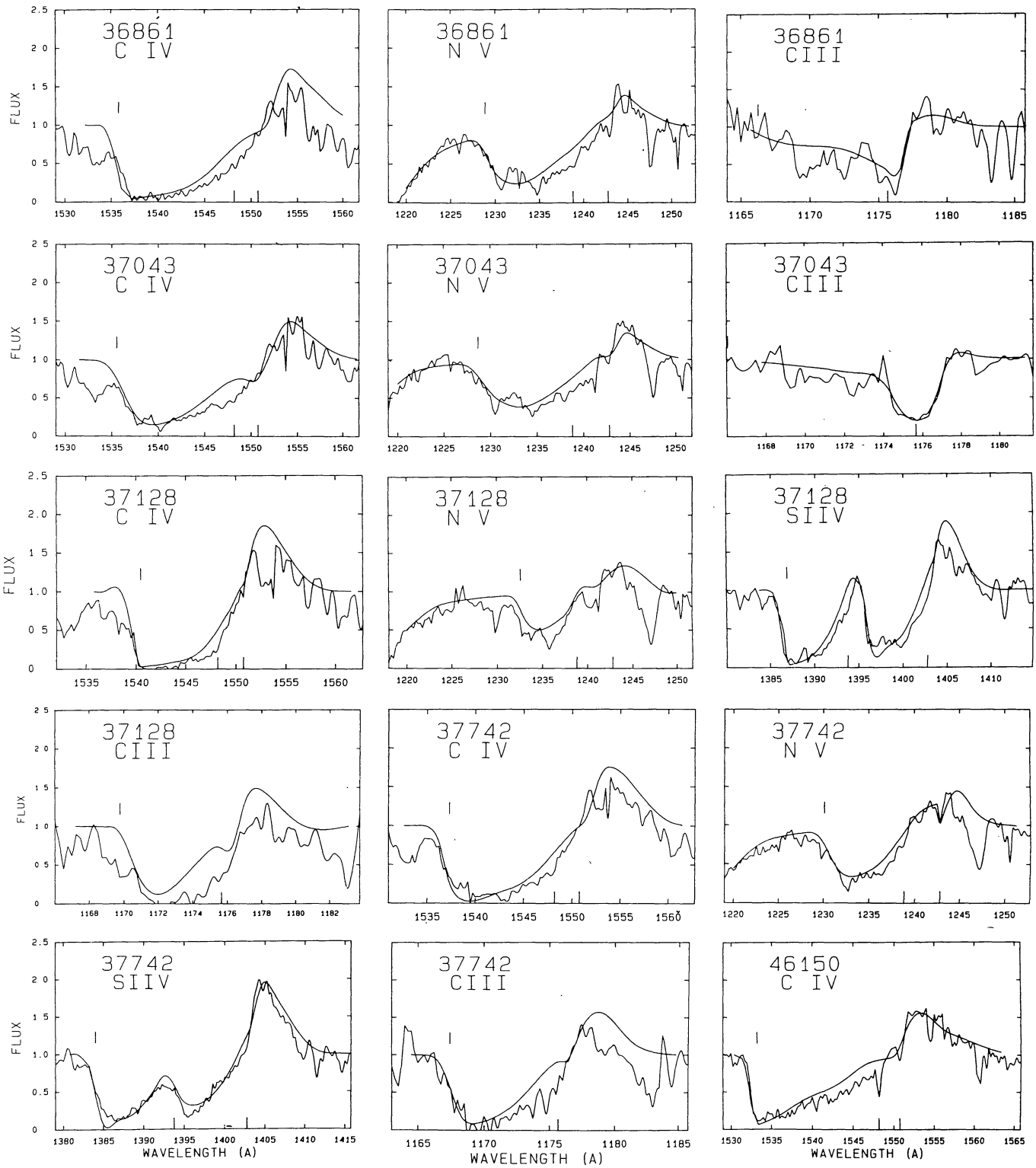

FIGURE 2b. — Same as figure 2a.

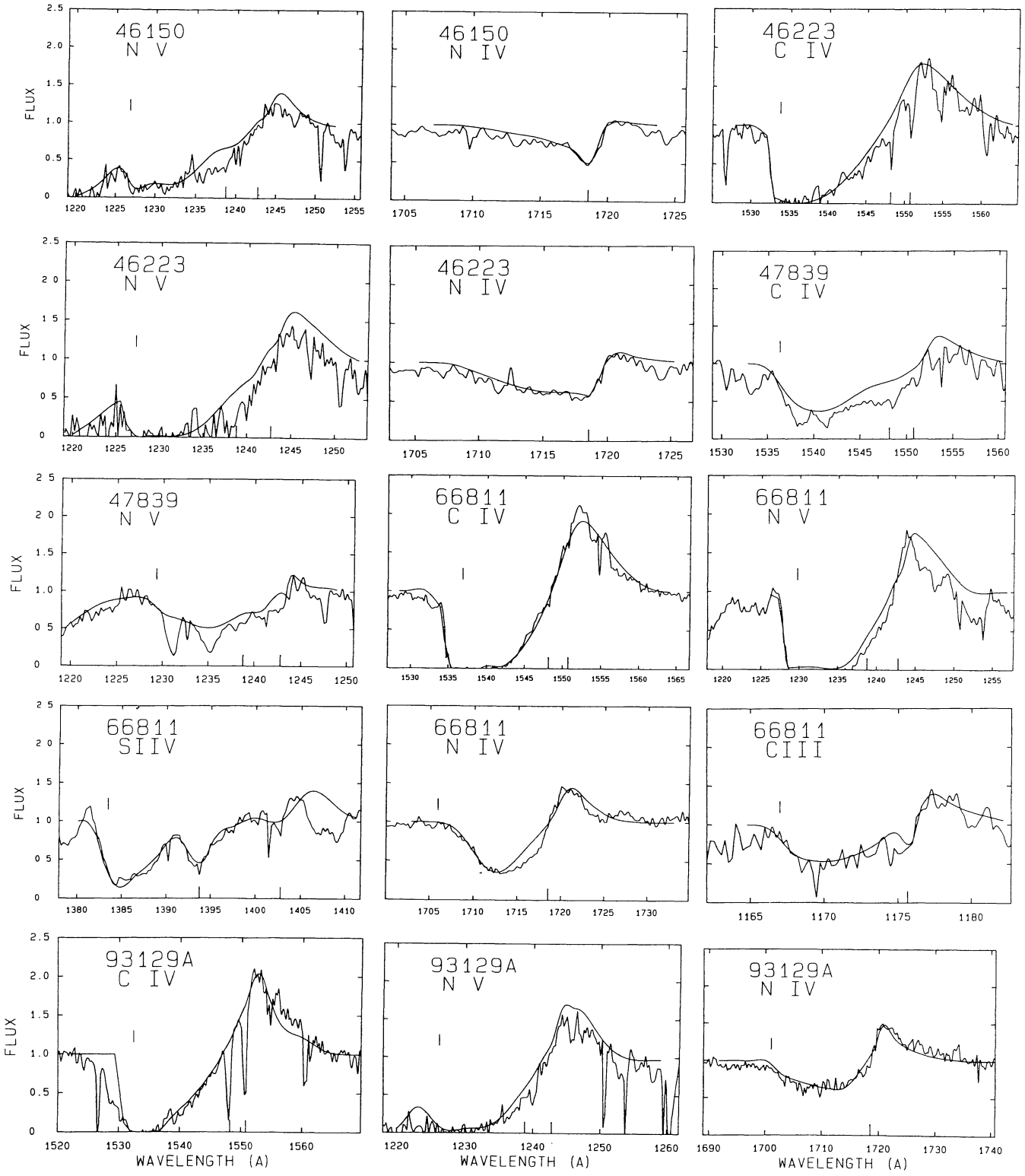

FIGURE 2c. — Same as figure 2a.

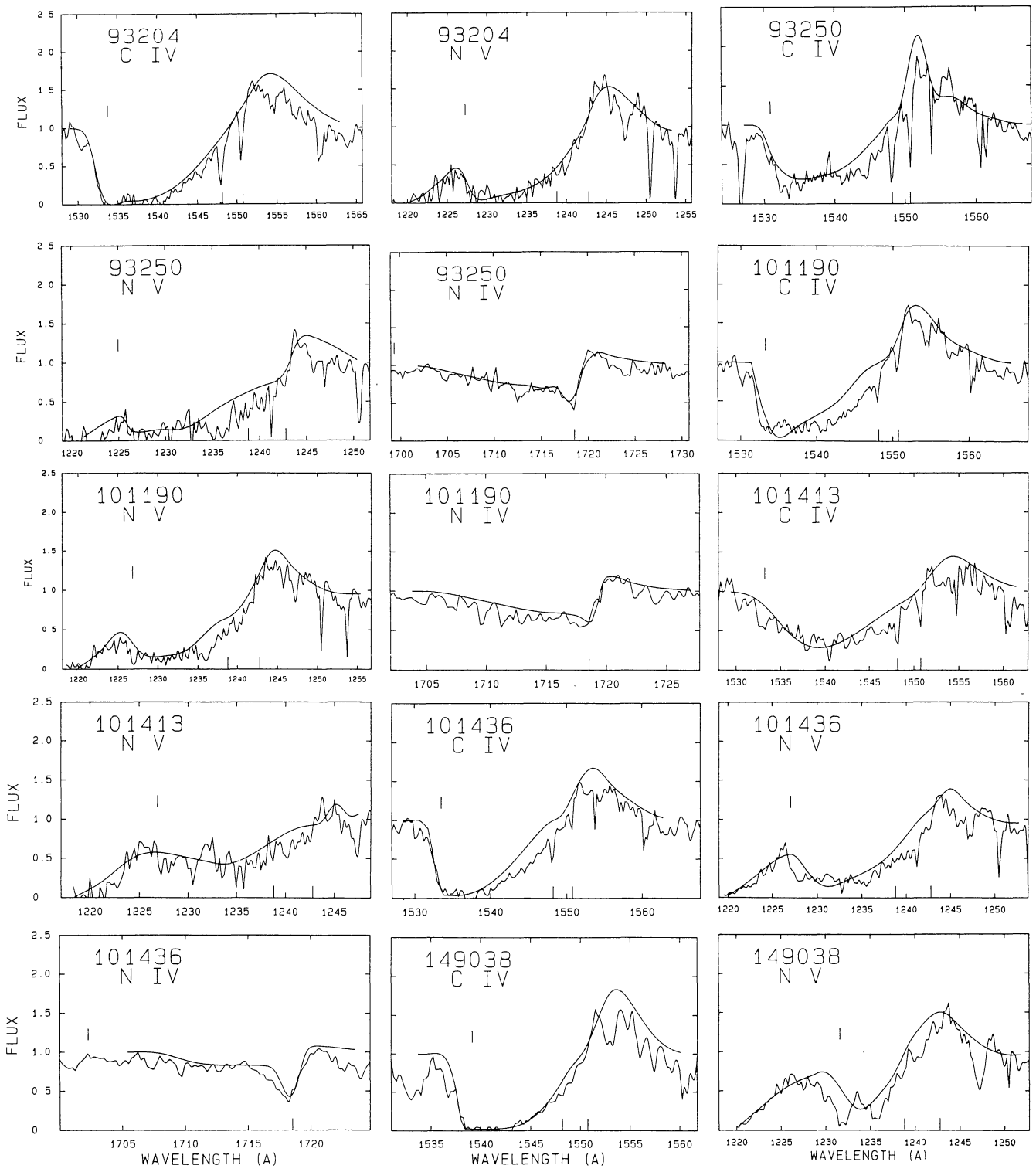

FIGURE 2d. — Same as figure 2a.

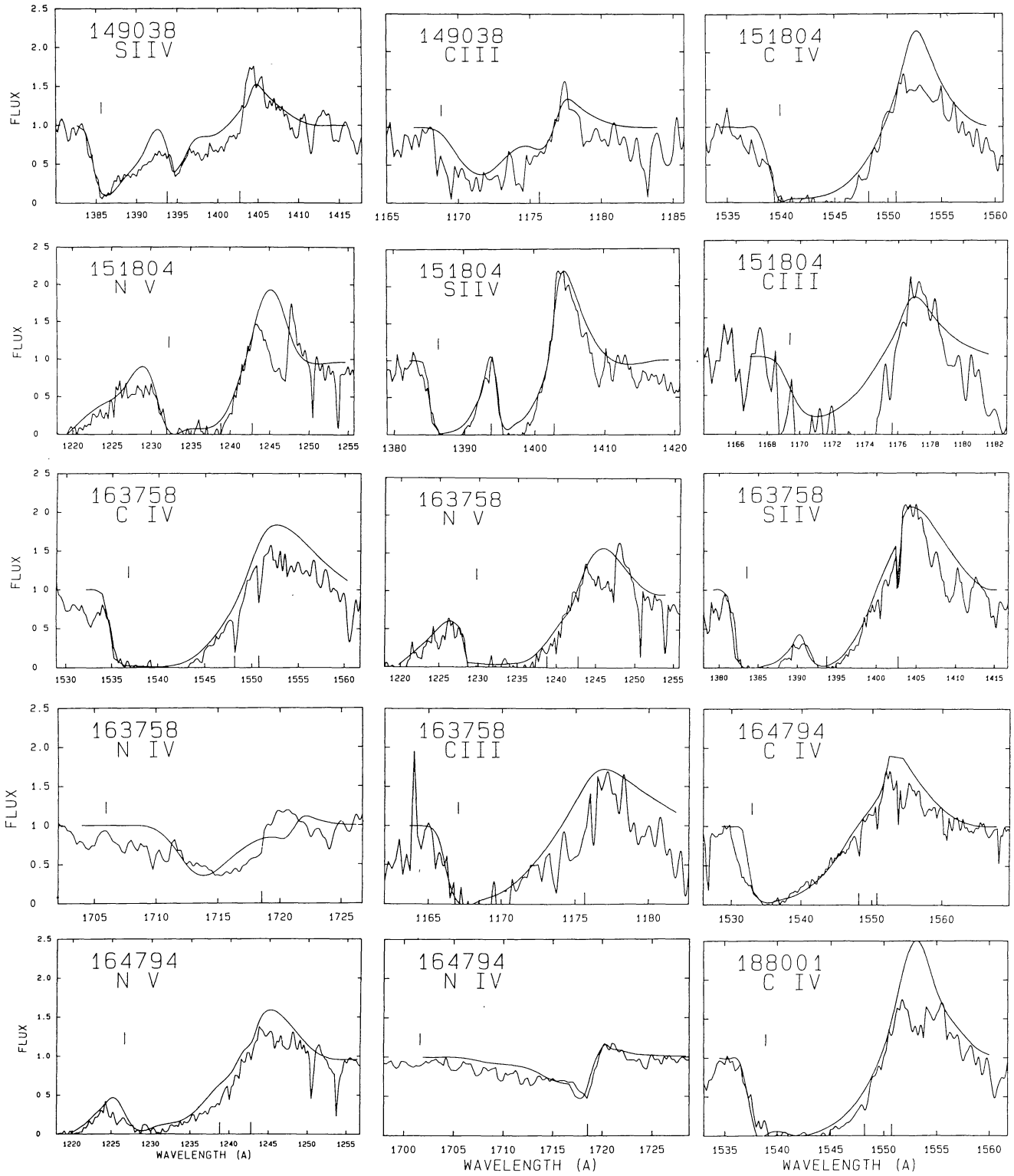

FIGURE 2e. — Same as figure 2a.

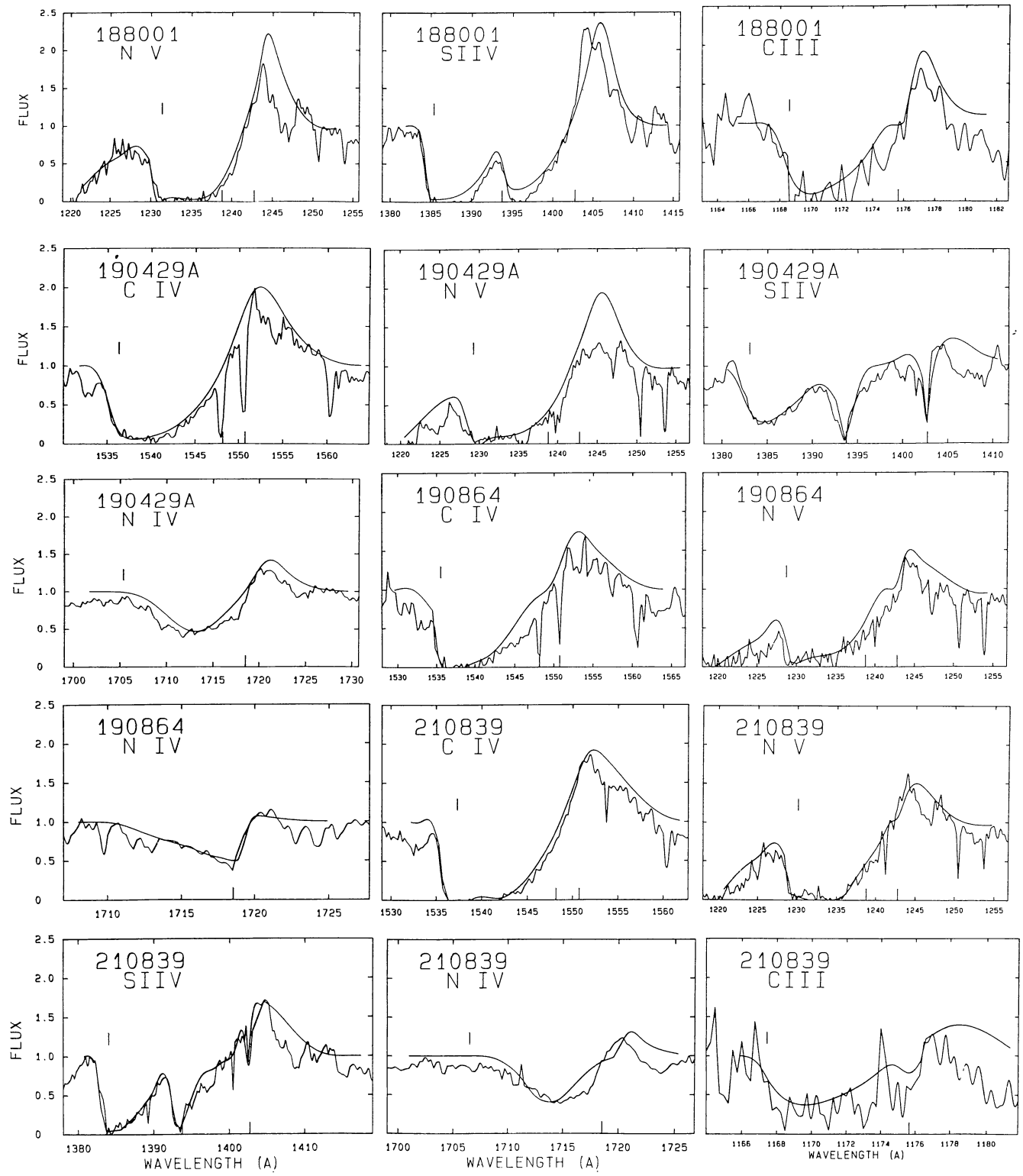

FIGURE 2f. — Same as figure 2a.

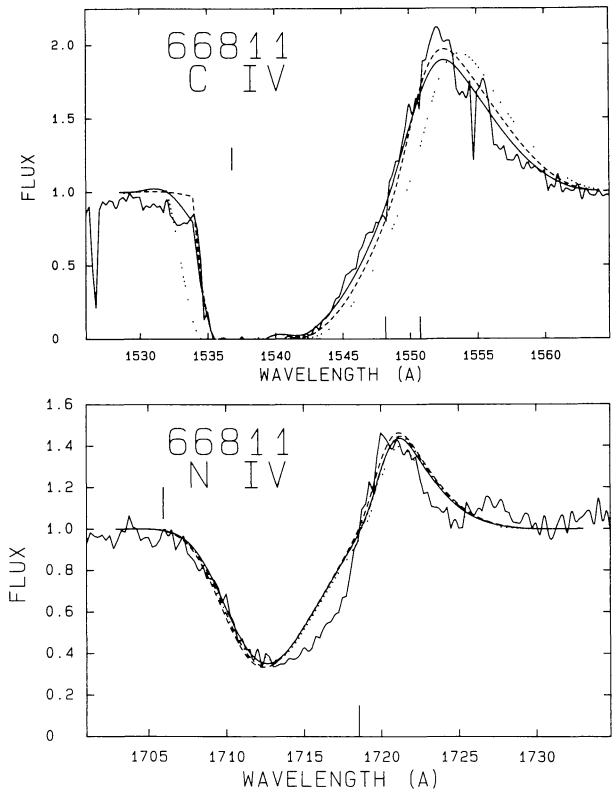

FIGURE 3. — The sensitivity of the predicted profiles to the adopted parameters is demonstrated by comparing the observed profiles of C IV (a) and N IV (b) of ζ Pup with theoretical profiles of different parameters. In both cases the jagged line is the observed profile and the full smooth line is the best-fit theoretical profile. The parameters of the theoretical C IV line are : (solid line) T_R= 7.2, α_1 = 0.97, v_{turb}= 290 km/s ; (dotted line) T_R= 65, α_1 = 0.97, v_{turb}= 290 km/s ; (dashed line) T_R= 65, α_1 = 2.0, v_{turb}= 200 km/s. The parameters of the N IV line are : (solid line) T= 2.3, α_1 = 0.4, α_2= 3.5 ; (dotted line) T= 2.3, α_1 = 0.4, α_2 = 4.3 ; (dashed line) T= 2.3, α_1 = 0.56, α_2= 3.5 ; (dashed-dotted line) T= 2.5, α_1 = 0.4, α_2= 3.5. A turbulent velocity of 290 km/s was assumed for the N IV line.

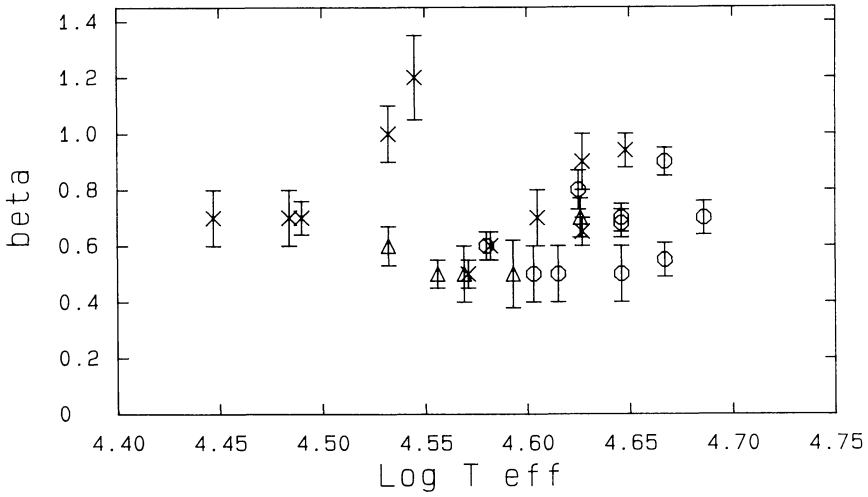

FIGURE 4. — The dependence of the velocity-law parameter β on T_{eff}. Luminosity classes are indicated by different symbols : circles = V, triangles = III, crosses = I. There is no clear correlation of β on T_{eff}. The mean value is $\bar{\beta} = 0.68 \pm 0.15$. The supergiants have slightly larger values of β than the main sequence stars.

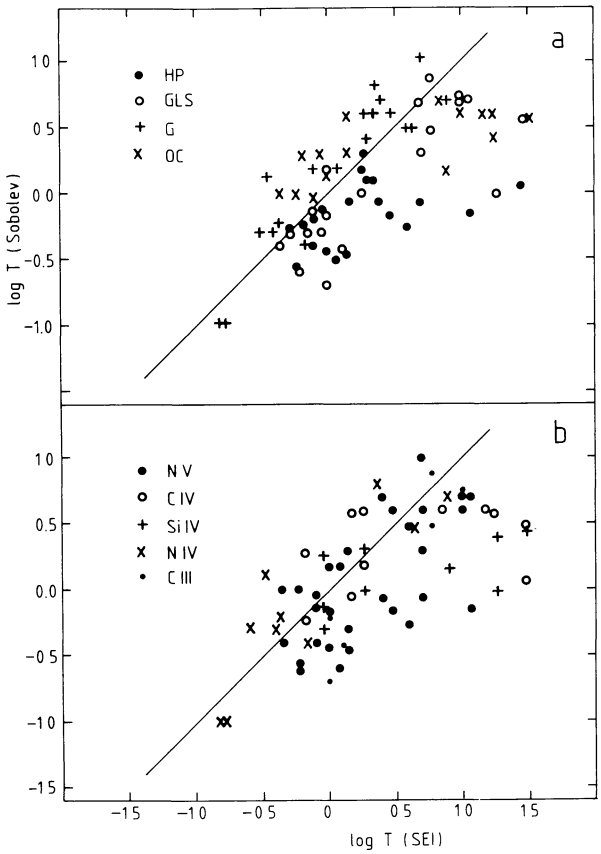

FIGURE 5. — The integrated optical depth T derived from line fits with the Sobolev approximation is compared with those derived with the SEI method used in this paper. The figure shows that the differences are large and of the order of 3 to 10^2. Figure A shows the results from different authors. There are large systematic differences between the results of different authors. Figure B shows the same data but differentiated according to the ions. There is no systematic difference between the results for the various ions. The origin of the large discrepancies is discussed in section 6.2.

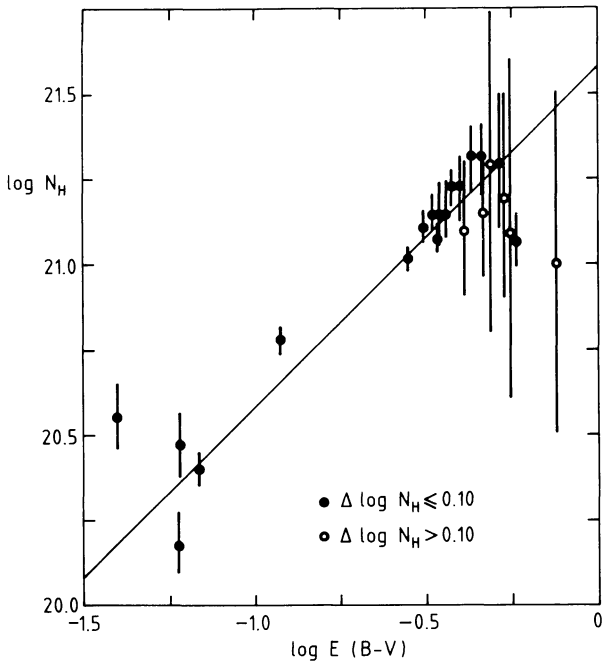

FIGURE 6. — The relation between the column density of neutral hydrogen (atoms/cm^2) derived from the Lα wings and $E(B-V)$ is shown. Filled symbols refer to the most accurate determinations of N_H. The mean relation is : $\log\{N_H/E(B-V)\} = 21.58 \pm 0.10$.